CHAPTER IV
RESULT AND DISCUSSION

4.1 PS/NR/MA blends Characterization

4.1.1 Torque study of PS/NR/MA Reactive blend

Temperature and torque profiles were recorded along blending step from Brabender Plasticorder. The temperature and torque profiles were shown in Figure 4.1.

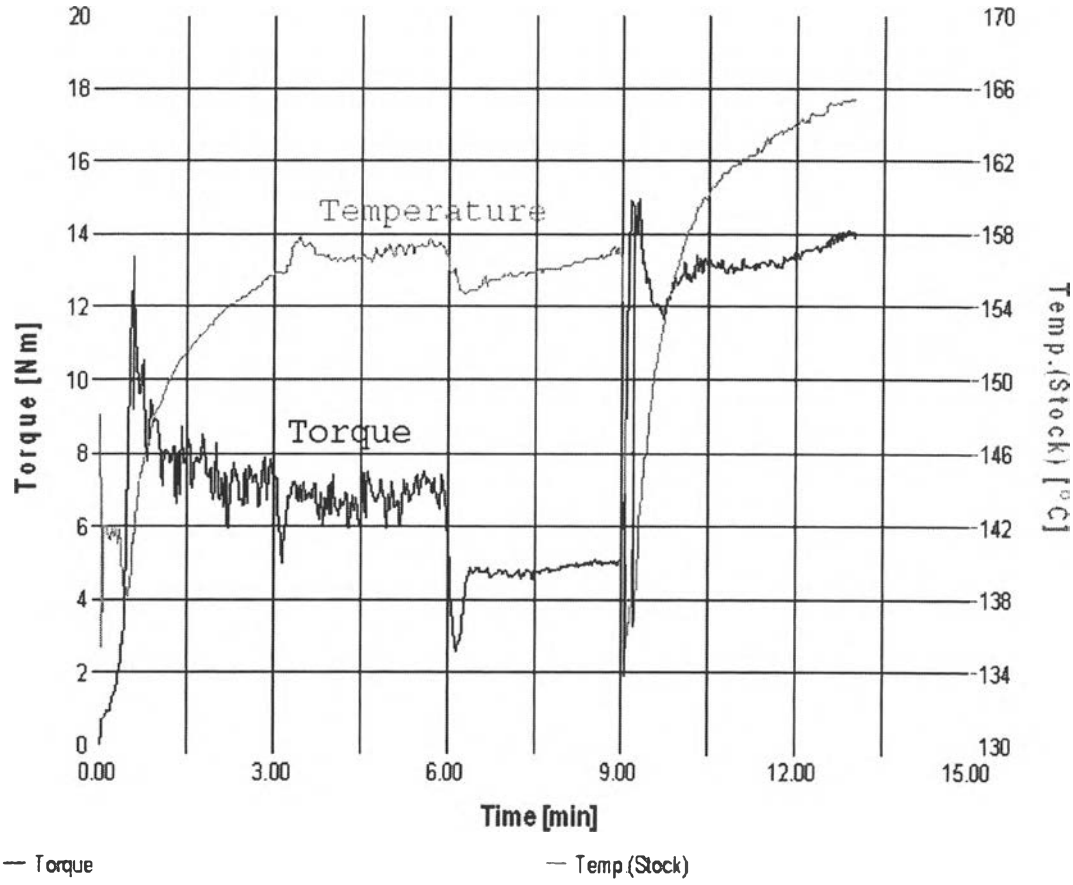

Figure 4.1 Temperature and torque profiles of PS/NR/MA reactive blend (50 rpm, 150° C).

From Figure 4.1, Brabender Plasticorder temperature started at 150°C and suddenly dropped when PS was added into the chamber due to cooling by PS pellets. Temperature slightly increased when DCP was added at 3rd minute and

MA at 6th minute indicating some reactions occurred to PS. When NR was added into the chamber at 9th minute, temperature suddenly dropped again due to cooling by NR and then increased again suggesting some reaction could be occurred.

Torque profile was recorded along blending process also. Torque increased when PS was added into the chamber and slightly decreased when DCP was added at 3rd minute. Especially, when MA was added, the torque reduced obviously with small increment of temperature indicating some chain scission occurred. When NR was added into the chamber, torque increased again since cross-linking reaction. The possible reactions are

At 3-6th minute $PS + DCP \rightarrow PS\cdot$ (1)

At 6-9th minute $PS + MA \rightarrow PS\text{-}g\text{-}MA$ (2)

$PS\cdot + MA \rightarrow PS\text{-}g\text{-}MA\cdot$ (3)

After 9th minute $NR + DCP \rightarrow NR\cdot$ (4)

$NR\cdot + NR\cdot \rightarrow$ crosslink NR (5)

$NR + MA \rightarrow NR\text{-}g\text{-}MA$ (6)

$NR\cdot + MA \rightarrow NR\text{-}g\text{-}MA\cdot$ (7)

$PS\cdot + NR\cdot \rightarrow$ NR-b-PS or NR-g-PS (8)

$PS\text{-}g\text{-}MA\cdot + NR\text{-}g\text{-}MA\cdot \rightarrow PS\text{-}gMA\text{-}NR$ (9)

The reactive blend with anhydride functional group prepared in this step was used as a reactive compatibilizer for Nylon12 and NR blend. The blend of Nylon12/NR at composition of 80/20 weight ratio was used as a blank in this work.

The temperature and torque profiles of PS/NR (with DCP at 3rd minute) blend were showed in Figure 4.2. Compared with PS/NR/MA reactive blend, torque profile of PS/NR blend is lower than another one at 13th minute. This is indicated that MA generated grafting reaction and resulted to increase torque due to the difficult of mobility of blend.

Temperature profile of PS/NR blend also decreased compared with PS/NR/MA reactive blend at 13th minute. This may be from no reaction generated along blending process so no heat generation.

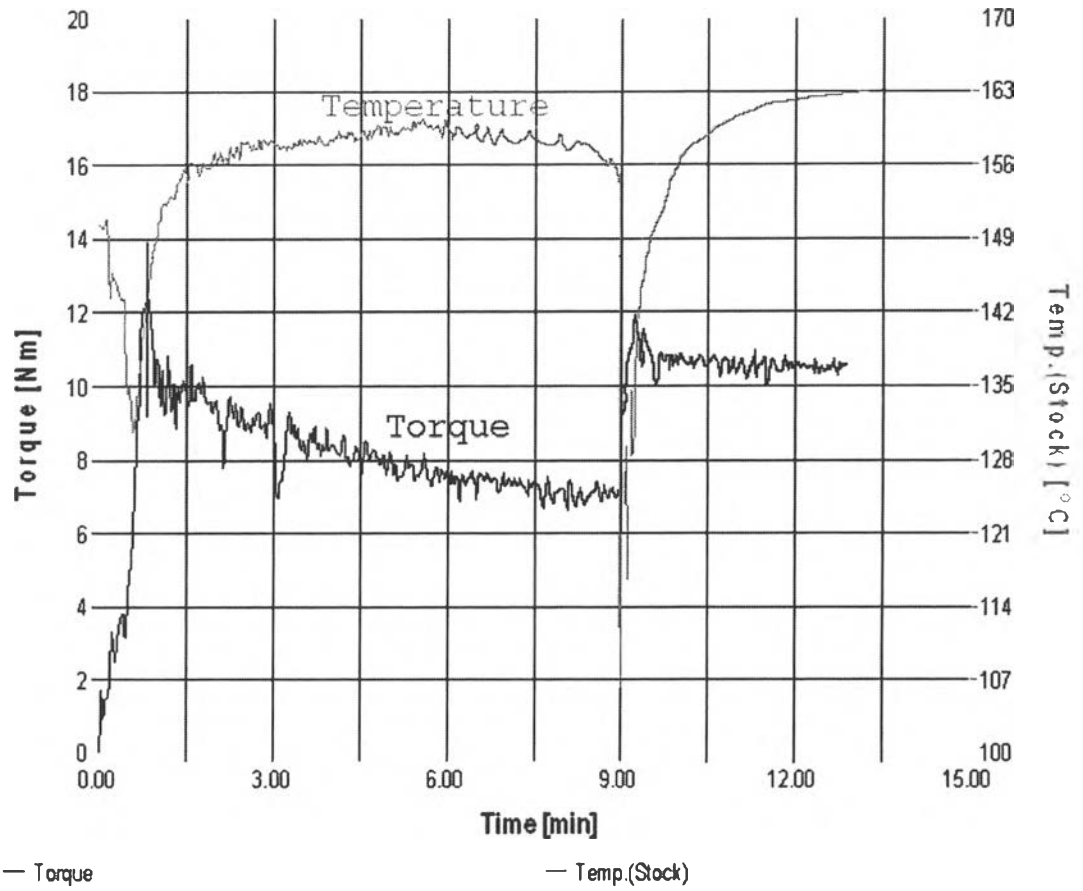

Figure 4.2 Temperature and torque profiles of PS/NR blend (50 rpm, 150° C).

From PS/NR/MA reactive compatibilizer blend, melt flow index was measured from the sample taken out from the mixer at several stage of mixing to study the reaction along blending step. The results were showed in Table 4.1.

Table 4.1 Melt flow index of PS and PS with DCP (at 3rd minute) and MA (at 6th minute) (200°C and 5 kg)

Polymer blend	Melt flow index (g/10 minutes)
Polystyrene	10.29
Polystyrene+Dicumyl peroxide	20.35
Polystyrene+Dicumyl peroxide+Maleic anhydride	41.77

From Table 4.1, polystyrene blended with dicumyl peroxide and polystyrene blended with dicumyl peroxide and maleic anhydride showed lower melt

flow index than polystyrene. This indicated that molecular weight of PS decreased and its chains had been scissioned when dicumyl peroxide and maleic anhydride were added. When NR was added to the reactive PS/DCP/MA, the reactions was extended with NR. Some side reaction like crosslinking may occur. This could be detected by the gel formation.

4.1.2 Gel content of PS/NR/MA reactive compatibilizer

Gel content of PS/NR/MA reactive compatibilizer was measured by swelling technique. Firstly, sample was dissolved in toluene (2% by weight) and stirred for 2 days to get complete dissolution, see Figure 4.3. Then, the blend solution was filtered by weighted filter paper (Whatman No. 1). Then, the wet filter papers containing gel were dried at 110°C for at least 5 hours to ensure steady dried weight. Finally, the filter papers with gel were weighted and %wt gel was calculated. From the experiment, the % gel content was 41.73%. This suggested that the crosslink reaction was intensive. The gel may be an interprenetrating network of NR/PS as well as the crosslinked NR.

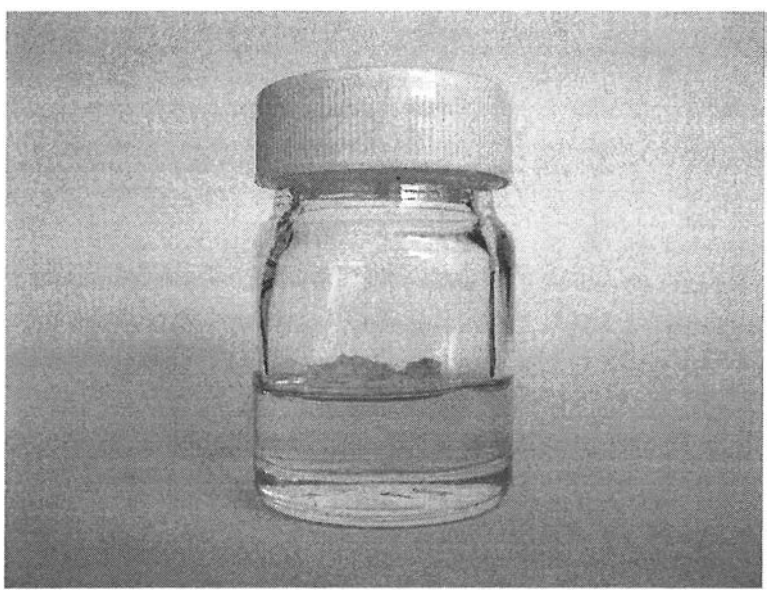

Figure 4.3 PS/NR/MA reactive blend dissolve in toluene.

4.1.3 Thermal Properties of PS/NR/MA blend

Glass transition temperature of blend was detected by differential scanning calorimeter (DSC) from -20°C to 200°C with heating rate of 10°C/min

under nitrogen purge. Figure 4.4 showed heat flow of PS/NR/MA reactive compatibilizer compared with temperature.

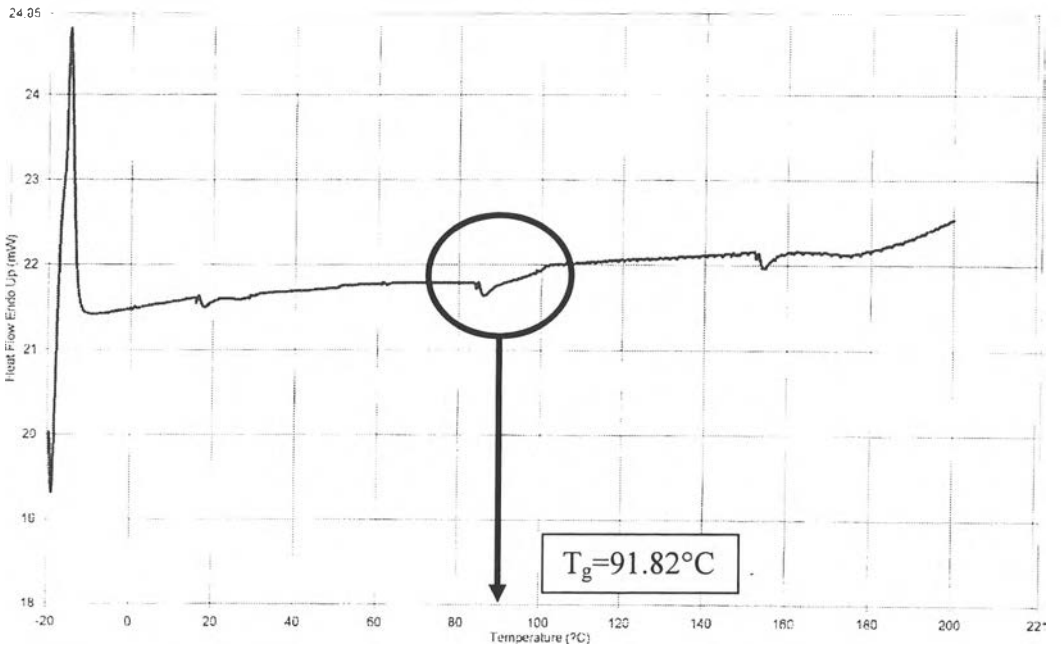

Figure 4.4 Heat flow of PS-NR-MA reactive compatibilizer.

The change of slope in Figure 4.4 at 91.82°C showed T_g of PS in PS/NR/MA blend. Generally, T_g of PS is around 80 °C and that of NR is much lower; however, the PS/NR/MA blend shows high T_g which is higher than expected. This is attributed to rigidity of the gel part. The endotherm peak around –15 °C may attribute to NR crystalline (glass transition temperature at –25°C, Kawahara *et al.*) or heat overshoot due to unstable morphology.

4.1.4 Determination of Content of Grafted Maleic Anhydride

By using solution carbon 13 NMR, the result in Figure 4.5 reveals that the content of PS and NR is approximately 58.29 and 38.75%wt (at chemical shift 120-130 ppm for PS and 20-40 ppm for NR). The amount of MA can be determined from the peak area at chemical shift of about 135 ppm which represents carbonyl carbon in MA. The grafted about is 2.48%wt.

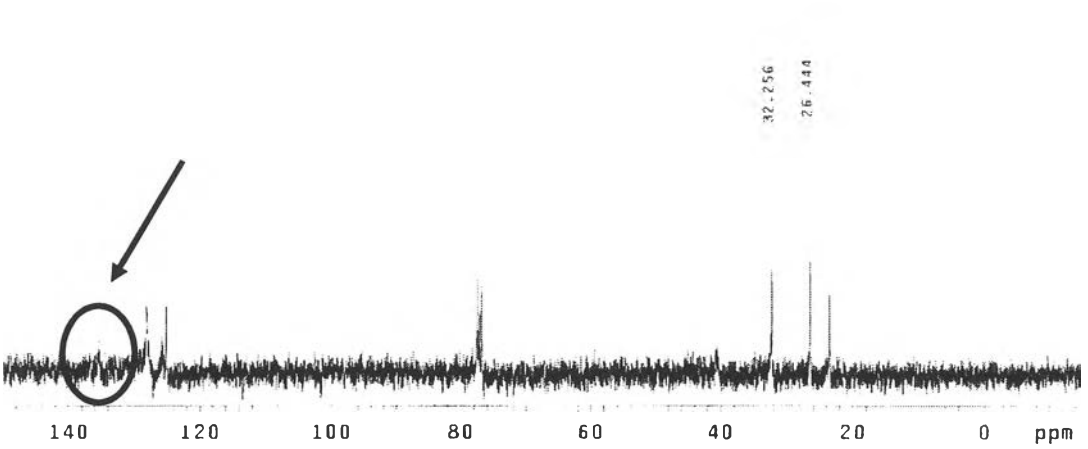

Figure 4.5 Carbon 13 NMR for PS/NR/MA using $CDCl_3$ as a solvent.

4.2 [Nylon12/NR]/[PS/NR/MA] Characterization

4.2.1 Torque study of [Nylon12/NR]/[PS/NR/MA]

Temperature and torque profiles were recorded along blending step from Brabender Plasticorder. The temperature and torque profiles were shown in Figure 4.6

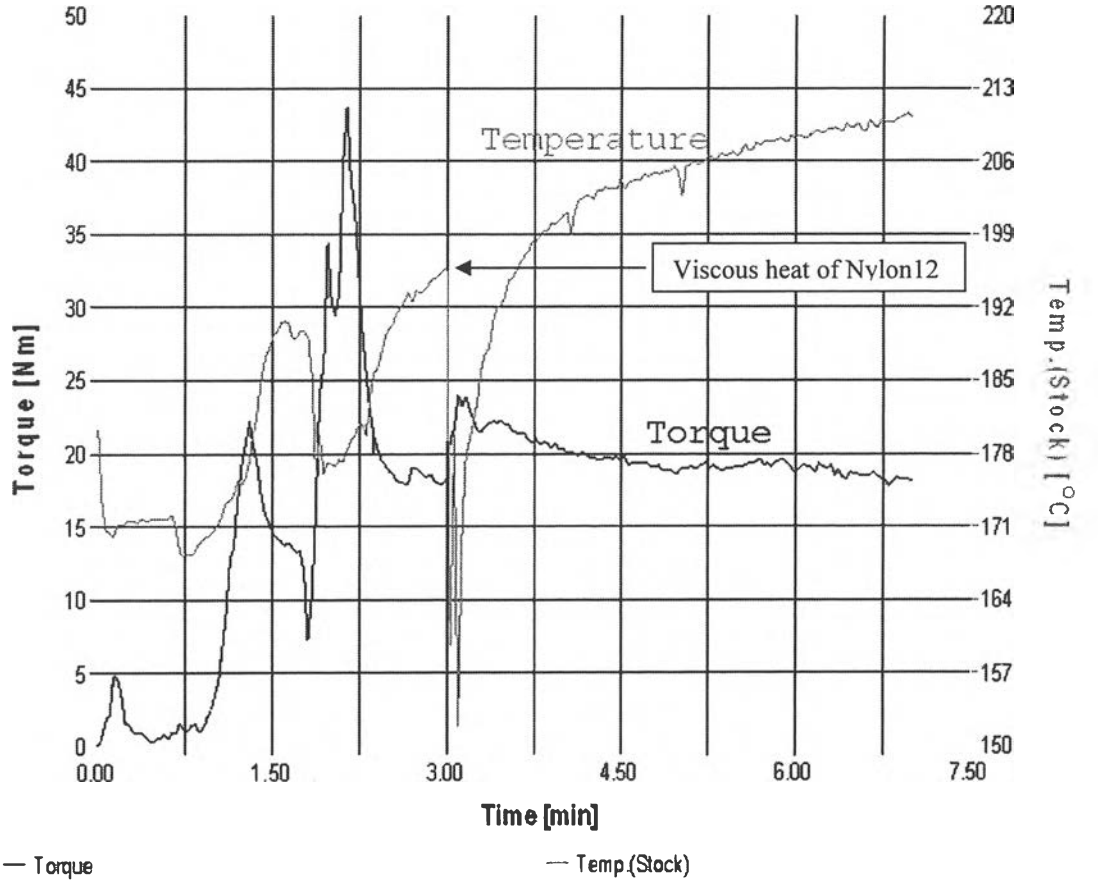

Figure 4.6 Temperature and torque profiles of [Nylon12/NR]/[PS/NR/MA] reactive blend.

From Figure 4.6, Brabender Plasticorder temperature started at 180° C and suddenly dropped when Nylon12 was added into the chamber for two steps (at 0 and 2nd minute) due to cooling by Nylon12 pellets. Temperature suddenly dropped when NR and compatibilizer were added at 3rd minute due to cooling by NR and compatibilizer then increased continuously until the end of process suggesting some grafting reaction could be occurred (about 30 °C total increments and about 15 °C above viscous heat of Nylon12).

Torque profile was recorded along blending process also. Torque increased when Nylon12 was added into the chamber for two steps (at 0 and 2nd minute) and slightly increased when NR and compatibilizer were added at 3rd minute suggesting the interaction occurred between Nylon12, NR and compatibilizer. Due to non-isothermal mixing (temperature keeps increasing), viscosity of the blend was

reduced with time and thus torque change was thus less obvious than temperature change.

4.2.2 Thermal Properties of Nylon12/NR/[PS/NR/MA] blend

Glass transition temperature (T_g) and melt temperature (T_m) of blend was detected by differential scanning calorimeter (DSC) from -20°C to 200°C. The blend was heated from -20°C to 200°C and then cooled to -20°C again under nitrogen purge. T_g and T_m were detected in second scan from -20°C to 200°C. Figure 4.7 showed heat flow of Nylon12/NR/[PS/NR/MA] reactive blend compared with temperature. It is noted that the heating range is above the glass transition of NR.

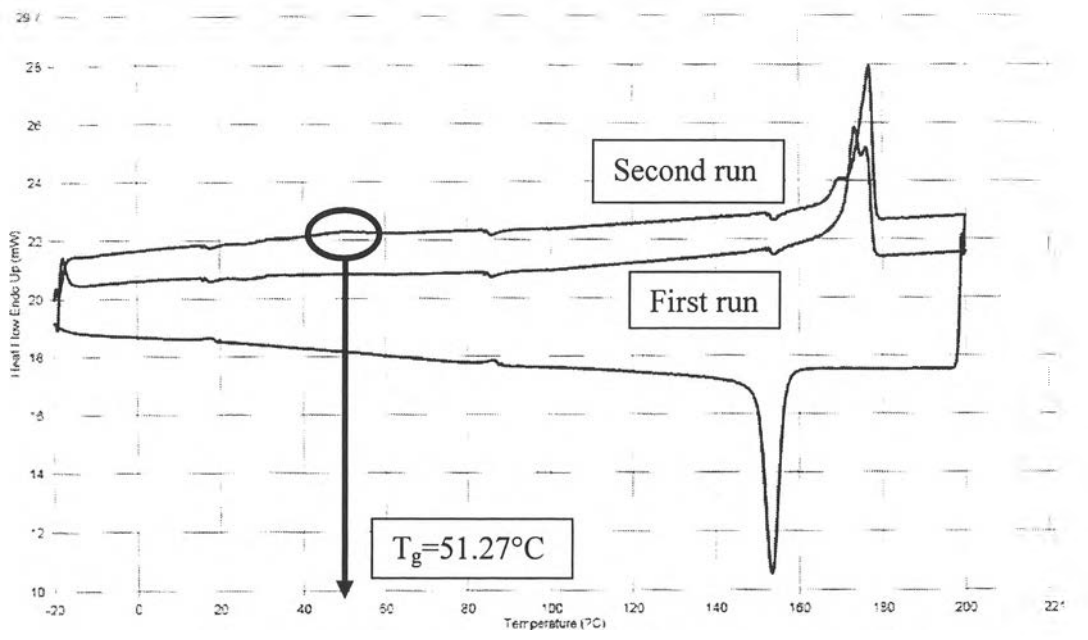

Figure 4.7 Heat flow of Nylon12/NR/[PS/NR/MA] blend.

From Figure 4.7, the peak at -18 °C was found like that in Figure 4.4 for the first run and then disappeared in the second run. This can conclude that this peak is due to the unstable morphology of sample and not the crystallinity of NR. The change of slope in Figure 4.7 at 51.27°C shows T_g of Nylon12 in Nylon12/NR/[PS/NR/MA] blend.

4.2.3 Crystallinity of Nylon12/NR/[PS/NR/MA] blend

Crystallinity in term of heat of fusion was observed by differential scanning calorimeter (DSC) from -20°C to 200°C for two steps. The heat of fusion for Nylon12 crystalline from the sample obtained from compression molding was observed as a first heating run (first heat of fusion) and the more equilibrium heat of fusion obtained from the sample from the second heating was also observed. Table 4.2 showed T_m, T_c, ΔH_f, and ΔH_c of [Nylon12/NR]/[PS/NR/MA] with various [PS/NR/MA] content. Moreover, Figure 4.8 showed heat of fusion from the first and second runs that vary with the content of compatibilizer. It is showed that by adding PS/NR/MA 16 phr the heat of fusion or crystallinity decreases by 40 % of the maximum (at 2 phr).

Table 4.2 T_m, ΔH_f, T_c, and ΔH_c of [Nylon12/NR]/[PS/NR/MA] with various [PS/NR/MA] content

[PS/NR/MA] content	T_m (°C) (1^{st} run)	ΔH_f (J/g) (1^{st} run)	T_c (°C)	ΔH_c (J/g)	T_m (°C) (2^{nd} run)	ΔH_f (J/g) (2^{nd} run)
1	176.83	33.97	153.47	34.22	173.20	35.04
2	177.67	35.54	152.30	36.89	176.87	36.94
4	176.67	38.02	152.63	39.02	176.53	38.63
8	176.33	31.55	153.30	31.96	173.03	32.95
16	175.50	23.15	153.30	23.65	172.70	24.35

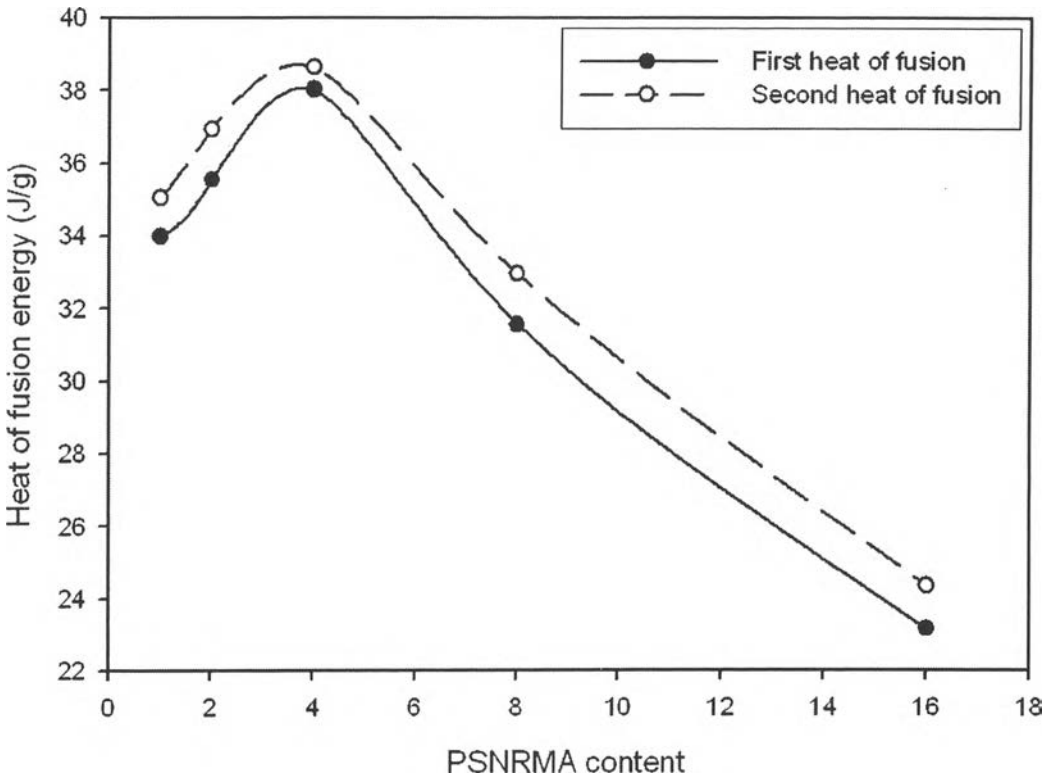

Figure 4.8 Heat of fusion of Nylon 12 crystalline in [Nylon12/NR]/[PS/NR/MA] with various [PS/NR/MA] content (from Nylon12 80% of blend).

From Figure 4.8, crystallinity increases initially and decreases continuously when compatibilizer content increases. At high compatibilizer content, low heat of fusion indicates low crystalline content resulting to lower mechanical properties (tensile properties and impact properties).

Therefore, [PS/NR/MA] blend prepared by reactive processing and containing gel can be used as a reactive compatibilizer in 80/20 %wt Nylon/NR blend. The following mechanical properties was obtained by adding [PS/NR/MA] at various amount in comparison with the non reactive compatibilizers, e.g. [PS/DCP/NR] and commercial grades of SEBS (G1650, 1652, and 1657), and the reactive one, e.g. SEBS-g-MA (FG1901X).

4.3 Mechanical Properties of [Nylon12/NR]/compatibilizer blend

4.3.1 The Effect of PS/NR/MA compatibilizer on the impact properties

Impact property was studied by Izod impact testing machine. The 21.6 J pendulum was used to test all specimens. All specimens were not broken as showed in Figure 4.9. The result of impact energy (not fully broken) was shown in Figure 4.10 also. From Figure 4.9, it is noted that the crack region is whitened. This indicates a special mechanism of deformation in the fast mode as also observed from the blends of polyamide6/polycarbonate compatibilized by SEBS-g-MA and combination of SEBS and SEBS-g-MA (Horiuchi et al., 1997)

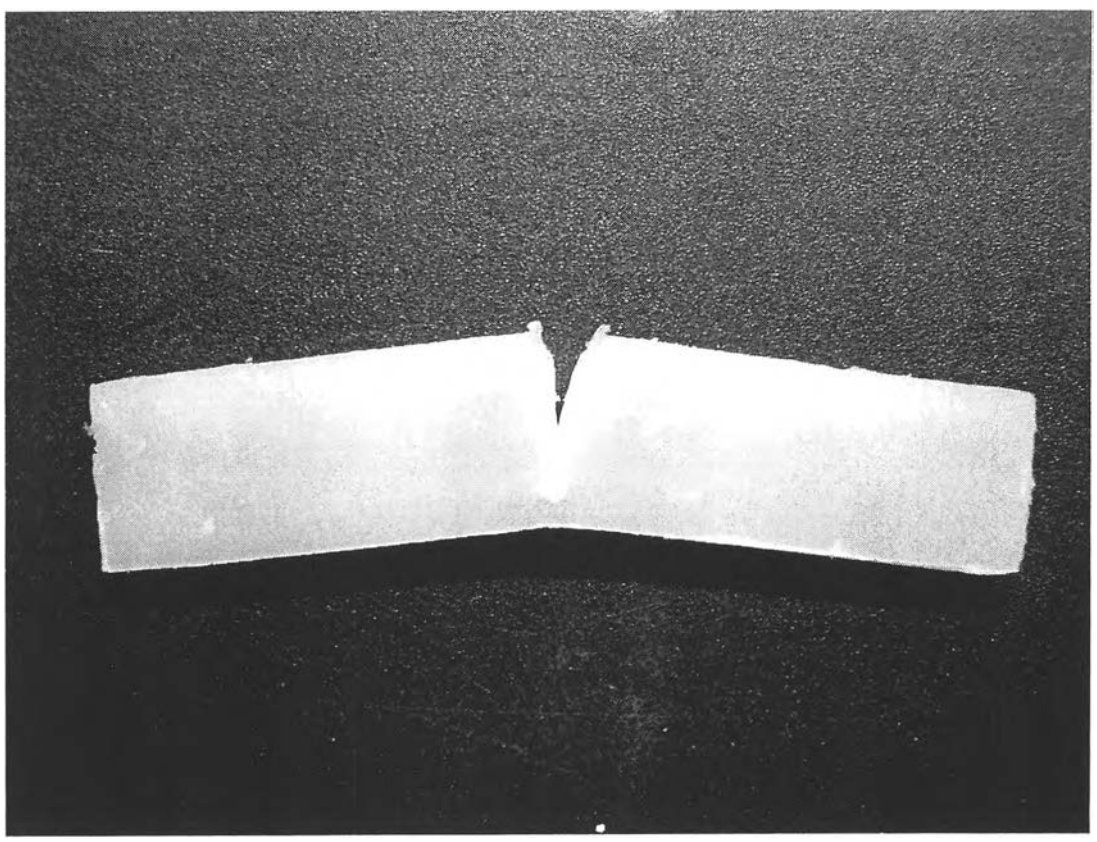

Figure 4.9 The tested specimen from Izod impact testing machine. Sample was not thoroughly broken into two pieces.

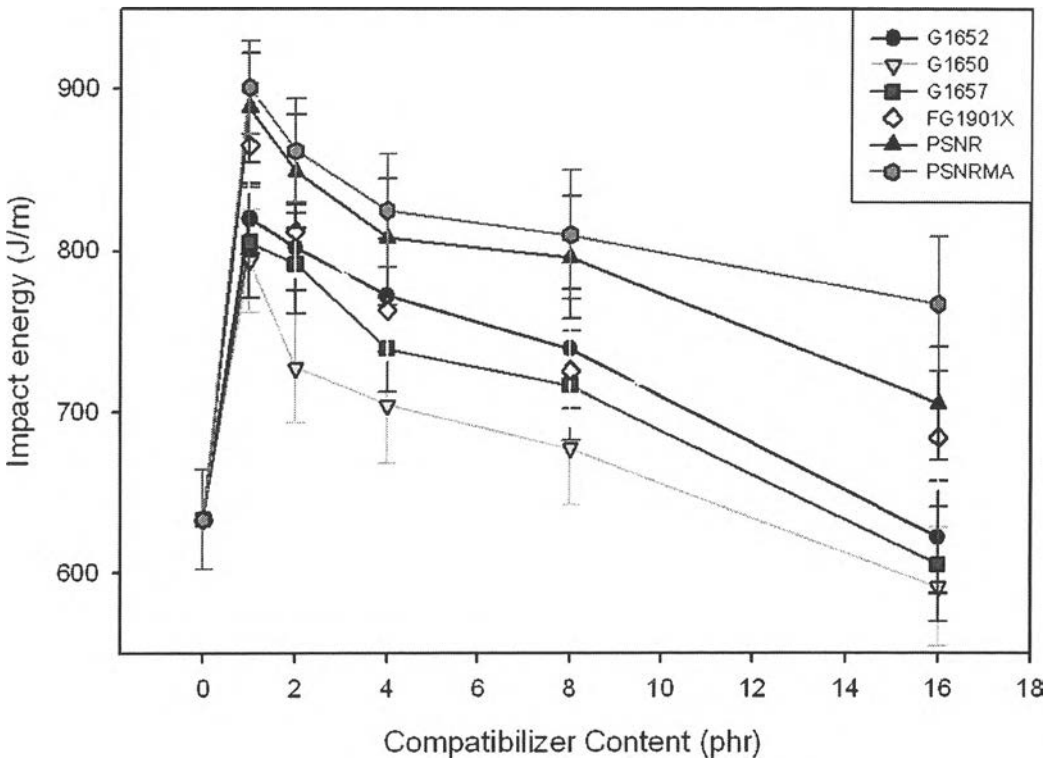

Figure 4.10 Impact energy of [Nylon12/NR]/Compatibilizer with 6 types of compatibilizer at various content of compatibilizer.

The effects of type of compatibilizer and compatibilizer content were shown in Figure 4.10. An 80/20 %wt Nylon 12/NR binary blend has impact strength of 633 J/m. With increase of the compatibilizer content in [Nylon12/NR]/ compatibilizer blends, the impact energy increased initially then decreased continuously. At very small content of compatibilizer (1-8 phr), the increase of impact energy can result from the suitable dispersed phase size, the strength of Nylon12 matrix, the flexible of NR, and proper morphology. The sequence of effective compatibilizer for impact strength improvement is [PS/NR/MA]>[PS/DCP/NR]>FG1901x>G1652>G1657>G1650. It is noted that all grades of non-reactive SEBS are not effective to improve impact properties at content 16 phr. The effectiveness to improve impact property of commercial reactive SEBS is poorer than the in-situ compatibilizers. It is noted that the content of the grafted MA in SEBS-g-MA and [PS/NR/MA] are nearly the same. Magaraphan *et*

al. (2004), showed that the blends with all commercial SEBS had lower crystallinity than that with [PS/DCP/NR]. Generally, impact strength is based on the amorphous part of the materials because its free structure can be altered to alleviate the imposed energy (better energy absorption than crystalline). However, the results are not related to the amorphous part of the blends (e.g. increasing compatibilizer content also increases amorphous content).

Horiuchi et al., 1997 reported that polamide6/polycarbonate (PA6/PC) blends with SEBS and SEBS-g-MA showed three different phase morphologies, core-shell (PC=core, PA6=matrix, SEBS-g-MA=core), stacking (blend with SEBS) and the intermediate between shell and stacking. According to this morphology, the samples showed whitening at crack region and the specimens were not fully broken. Magaraphan *et al.*, 2004 also showed that the morphology of Nylon12/NR/SEBS or SEBS-g-MA or [PS/DCP/NR] was core-shell type or the mixture of core-shell and stacking or intermediate. In fact, the SEBS-g-MA causes the simple morphology of NR core and compatibilizer shell and their stacking. Especially for non-reactive compatibilizer, not only NR but also Nylon12 was found to be the core surrounded by triple compatibilizer/NR/compatibilizer shells (so called complex core-shell) or Nylon12 inclusions in NR domains with compatibilizer shell. The complex core-shell may be occurred due to less viscous of the matrix than the dispersed phase such that shearing can overcome surface tension of the matrix and make small droplets of the matrix encapsulated by dispersed phase. The characteristics of non-reactive and reactive compatibilized morphology is that the former has increased particle size with compatibilizer content e.g. the dispersed phase size of [Nylon12/NR]/SEBS G1652 blends was increased with increasing the SEBS content but the later shows stabilized size once the optimum compatibilizer content is reached. In case of [PS/NR/MA], the dispersed particle size increases with compatibilizer content as shown by SEM micrographs in Figure 4.11 and a plot in Figure 4.12. This suggests that [PS/NR/MA] induces the complex core-shell or inclusion morphology rather than simple core-shell with minimized particle size as that found for the blends with SEBS-MA. The dispersed phase size was the greatest compared with other compatibilizers. The shape of the dispersed phase is irregular and becomes more spherical for the blends after addition of 1 phr SEBS. The

number average of dispersed phase size measurement was estimated by averaging the diameter of about 100 domains randomly for each blend system.

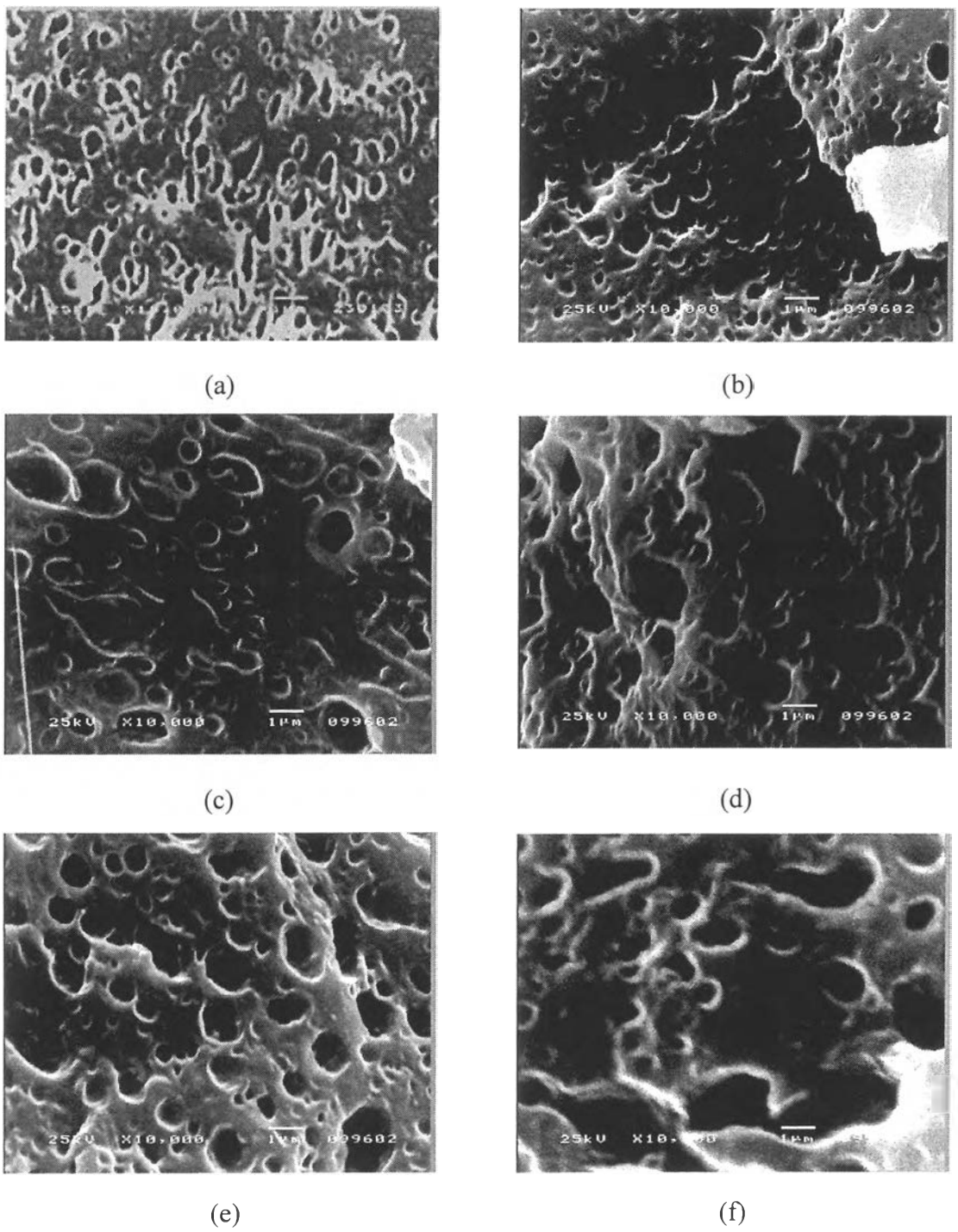

Figure 4.11 SEM micrographs of the cryofracture surface of the [80/20] [Nylon12/NR] blends at various [PS/NR/MA] content (a) 0 phr, (b) 1 phr, (c) 2 phr, (d) 4 phr, (e) 8 phr, and (f) 16 phr.

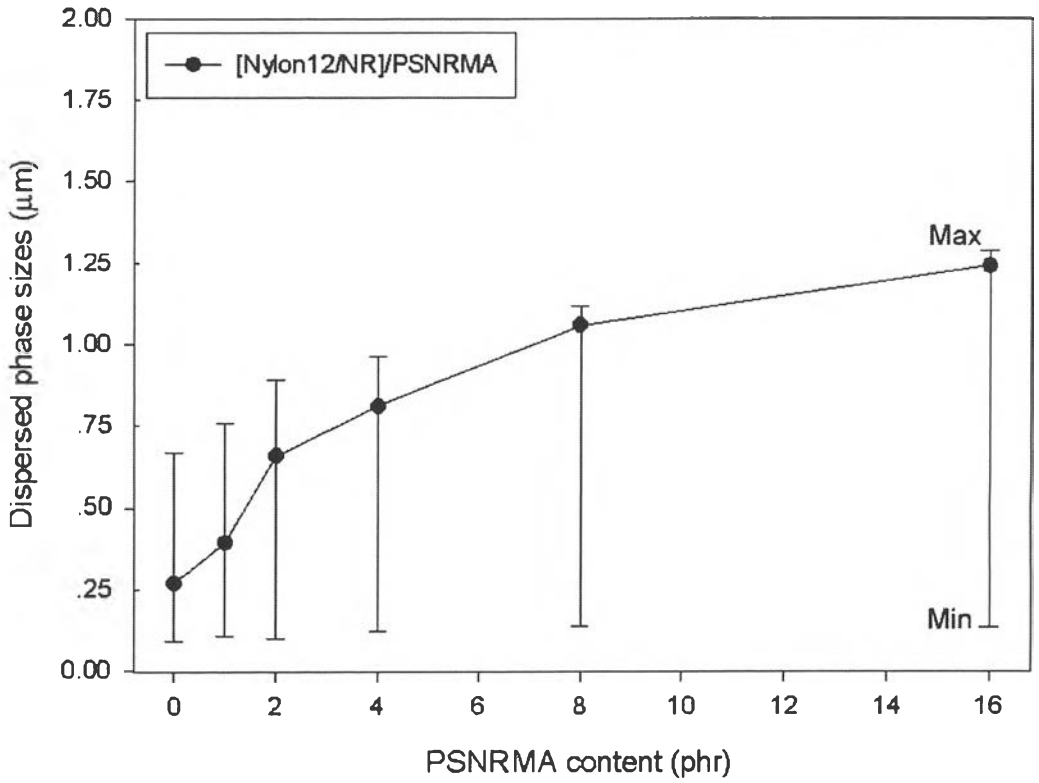

Figure 4.12 Dispersed phase size and distribution of [Nylon12/NR]/PS/NR/MA reactive blends with various PS/NR/MA content.

The mechanism of improved impact strength as found by Horiuchi *et al.*, 1997 for the similar compatibilizers was due to the void formation at the interface of the domain and matrix where encapsulation was not completed and this promoted the energy dissipation. In our case, the crack and whitening may occur by similar mechanism. The lowering of impact energy with increasing compatibilizer amount was probably due to the coarser morphology or the broader dispersed size in Nylon12 matrix. With various type of compatibilizers in [Nylon12/NR]/ compatibilizer blends, PS/NR/MA compatibilizer act as the best compatibilizer compared with others probably attributed to the higher NR content (40% wt) and have MA which is the reactive reagent to Nylon12. Moreover, the gel in PS/NR/MA may benefit to the energy absorption in comparison to SEBS or SEBS-MA which have no gel.

4.3.2 The Effect of PS/NR/MA compatibilizer on the tensile properties

The effect of PS/NR/MA compatibilizer on the tensile stress was shown in Figure 4.13. The [Nylon12/NR]/PS/NR/MA showed a slightly higher tensile stress than FG1901X and PS/NR compatibilizer. However, at high [PS/NR/MA] content, the tensile stress of this blend was lower than those blends with FG1901X and PS/NR. In other words, at high loading, SEBS-MA is more effective to provide strong bonding at the interface than [PS/NR/MA]. This might be caused by the increasing gel content to obstruct the interaction between two phases. Tensile force causes the stretching of the matrix in combination with the voiding at the interface.

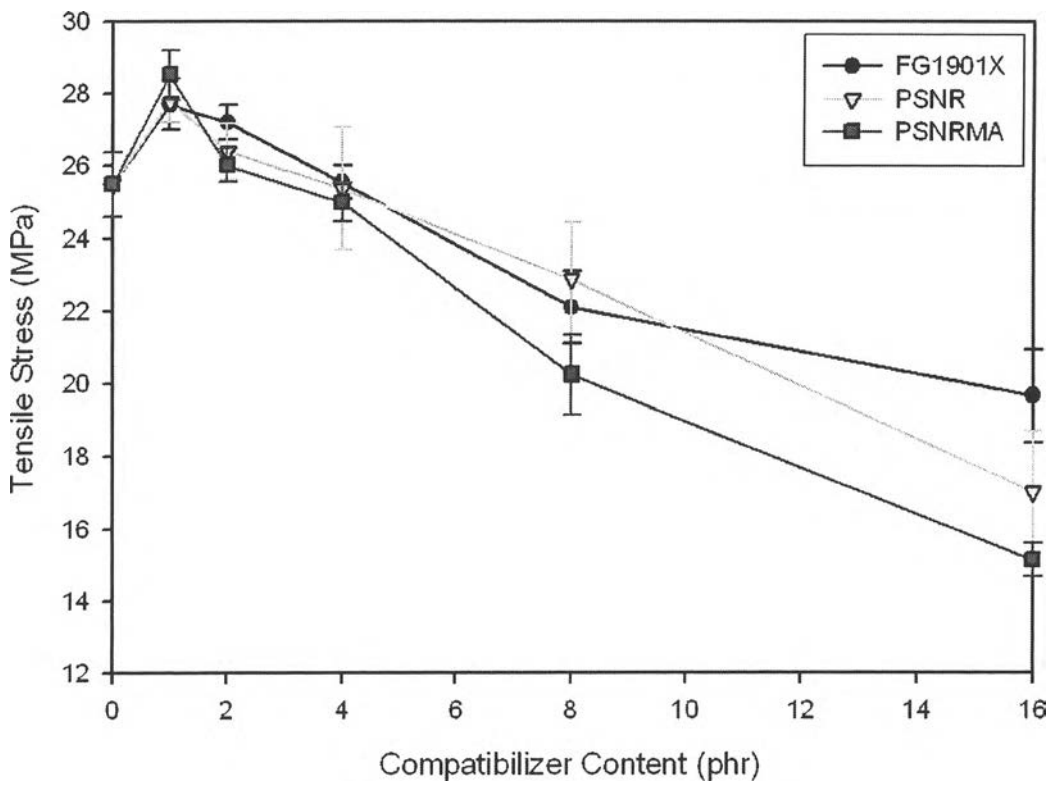

Figure 4.13 Effect of compatibilizer content on tensile stress of [Nylon12/NR]/compatibilizer blends with various content of PS/NR/MA in comparison to PS/NR and FG1901X.

The [Nylon12/NR]/PS/NR/MA showed a substantially higher tensile modulus than [Nylon12/NR]/PS/NR and [Ntlon12/NR]/FG1901X at low compatibilizer contents, as shown in Figure 4.14.

In summary,[PS/NR/MA] contained maleic anhydride which provided specific interaction to Nylon12 matrix. Maleic anhydride improves the morphology and mechanical properties at low compatibility contents.

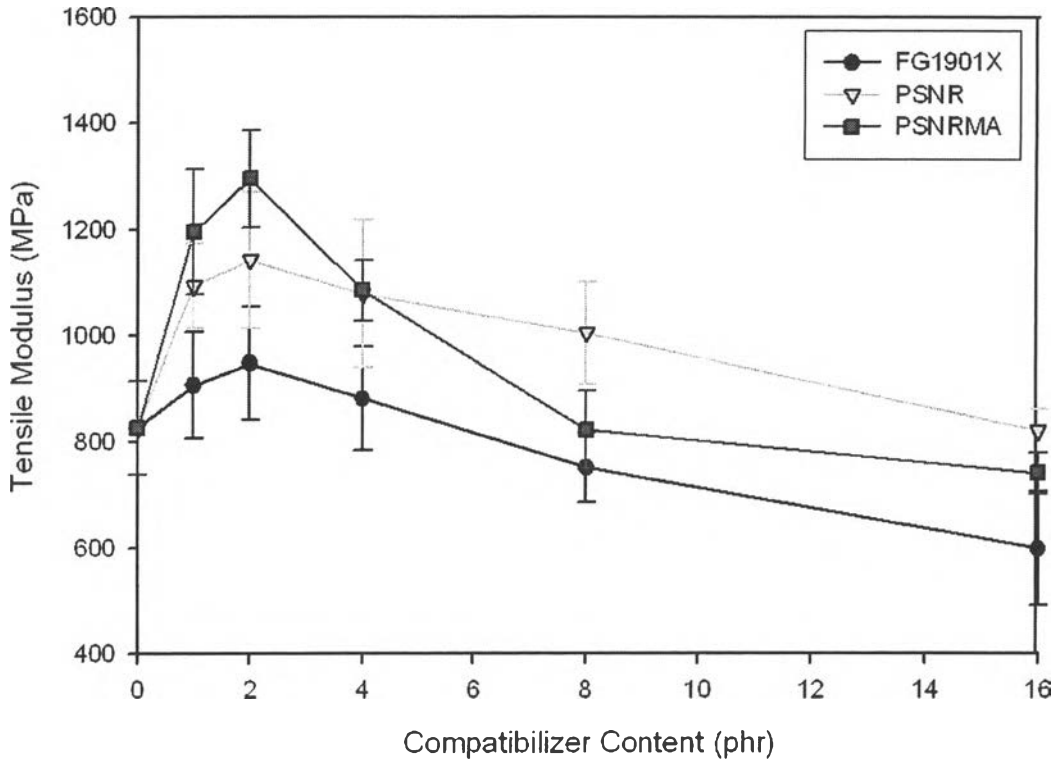

Figure 4.14 Effect of compatibilizer content on tensile modulus of [Nylon12/NR]/compatibilizer blends with various content of PS/NR/MA in comparison to PS/NR and FG1901X.

4.4 Dynamic mechanical characterization for [Nylon12/NR]/compatibilizer blends

Dynamic mechanical properties is a good measurement of molecular mobility based on viscoelasticity of the molecules. The work has been carried out for the solid state mechanical properties, storage and loss moduli and their ratio (tan δ) of the blends with various compatibilizers. The fast mode

response was observed at high frequency or low temperature (solid like response) and the slow mode response was observed at low frequency or high temperature. The blends with only 2 phr compatibilizers which showed an optimum properties were selected for the study.

4.4.1 Effect of Temperature in [Nylon12/NR]/compatibilizer blends

The effects of temperature on storage modulus, loss modulus and tan δ were shown in Figures 4.15, 4.16, and 4.17, respectively. These figures were obtained from [Nylon12/NR]/[PS/NR] non-reactive blend with [PS/NR] content of 2 phr. Storage modulus and loss modulus vary strongly with temperature within 30 °C to 70 °C and are less different at higher temperatures. With increasing temperature, storage modulus decreases obviously since the materials have more flexibility. Loss modulus and tan δ increased initially and decreased continuously when temperature increased. The increasing tan δ occurred near 50°C and 80°C (around frequency 1 rad/s) as a result of T_g of Nylon12 and PS, respectively. Both storage and loss moduli increased at high frequency and low temperature indicating the enhanced rigidity and relaxation simultaneously. Within the testing range storage molulus and loss modulus are different by one order of magnitude.

The storage modulus at low frequency has the lowest value compared with those at other frequencies due to longer time for the movement of the chain. At high frequency, the blend showed higher storage modulus due to less time available for the molecules to have some movement (becoming more solid-like). Moreover, at high temperature, frequency did not affect storage modulus so much because to the movement occurred easily compared with low temperature.

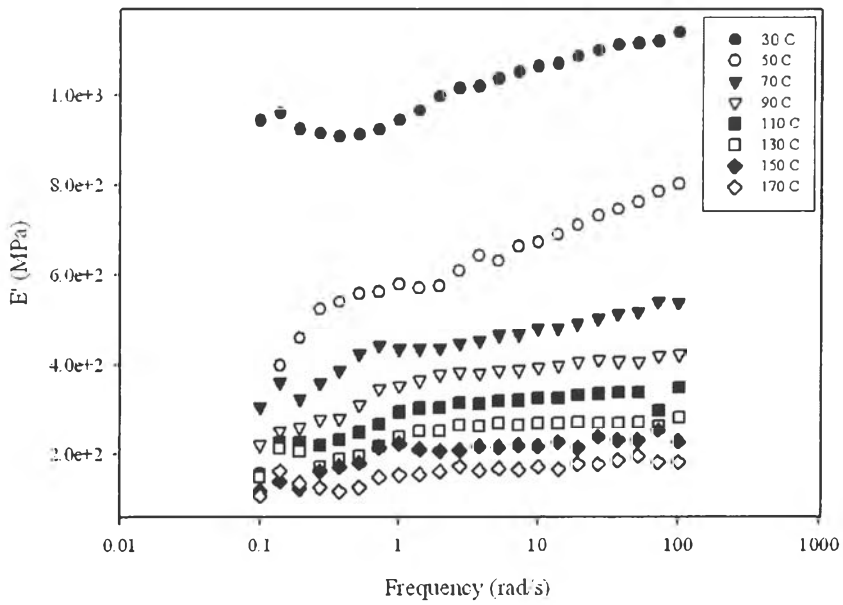

Figure 4.15 Storage modulus of [Nylon12/NR]/[PS/NR] with [PS/NR] 2 phr content reactive blend at various temperature.

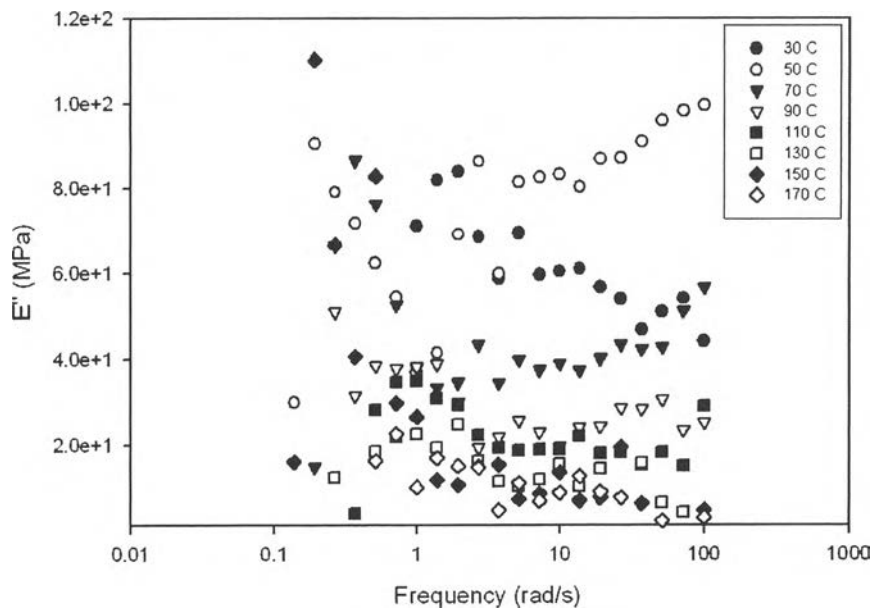

Figure 4.16 Loss modulus of [Nylon12/NR]/[PS/NR] with [PS/NR] 2 phr content reactive blend at various temperature.

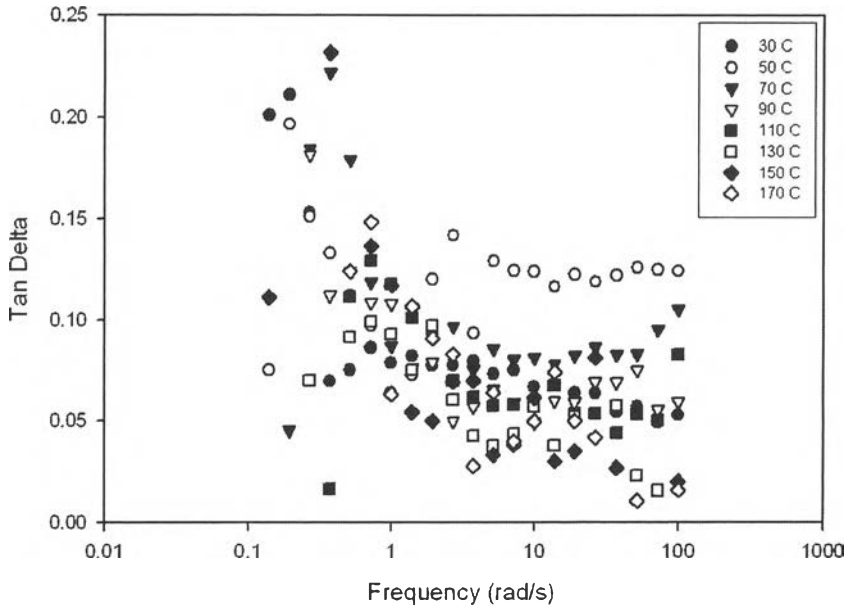

Figure 4.17 Tan δ of [Nylon12/NR]/[PS/NR] with [PS/NR] 2 phr content reactive blend at various temperature.

Figures 4.18, 4.19, and 4.20 showed the effects of temperature on storage modulus, loss modulus and tan δ of [Nylon12/NR]/[PS/NR/MA] reactive blend with [PS/NR/MA] content of 2 phr, respectively. PS/NR/MA compatibilizer showed the same result as PS/NR ; ie , storage decreased with temperature as well as tan δ since the materials have more flexibility. Storage modulus increased with frequency, especially at 30-70 °C while loss modulus acted differently depending on temperature and frequency. The loss modulus was large at 30 °C and low frequency and dropped fast to a plateau for the intermediate to high frequency. This suggests a more stable morphology. At higher temperature, the loss modulus increased with frequency as a result of more relaxation of Nylon 12 above its T_g. Tan δ was thus higher with temperature and energy loss was promoted at high frequency, 100 rad/s.

In comparison to the blend with PS/NR, similar results were obtained but with lower values. Storage modulus of the blend with PS/NR/MA at various temperatures were higher while loss modulus were higher at 30 °C and low frequency (less than 1) and became comparable at higher temperatures and frequency. Interestingly, the loss modulus of the blend with PS/NR/MA was lower

than that wit PS/NR at higher temperature and low frequency. This suggests that the specific interaction between MA and Nylon can suppress the long term motion of the molecules.

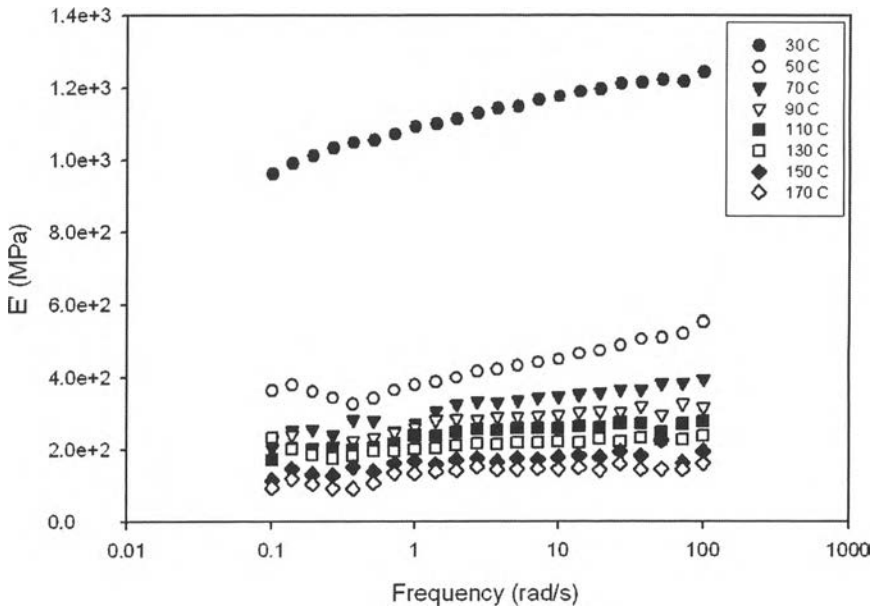

Figure 4.18 Storage modulus of [Nylon12/NR]/[PS/NR/MA] with [PS/NR/MA] 2 phr content reactive blend at various temperature.

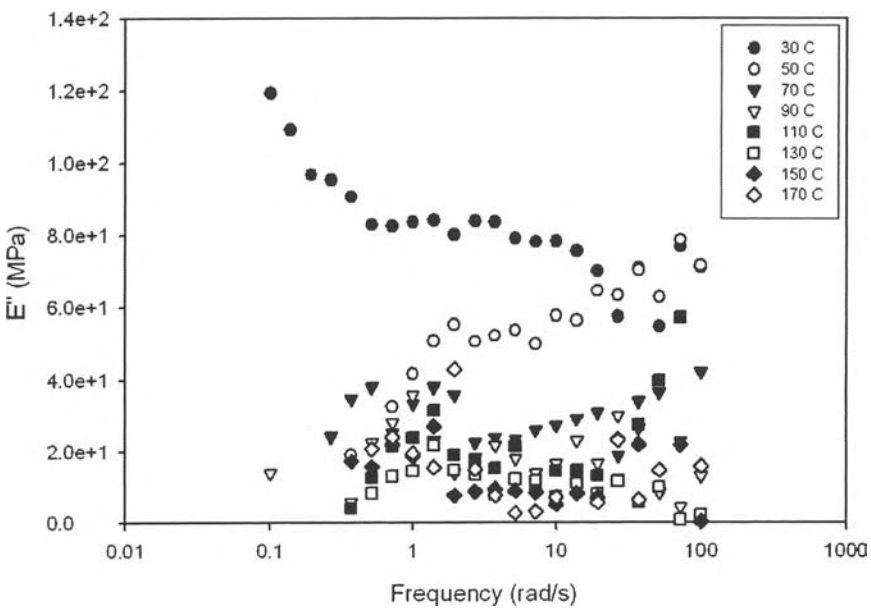

Figure 4.19 Loss modulus of [Nylon12/NR]/[PS/NR/MA] with [PS/NR/MA] 2 phr content reactive blend at various temperature.

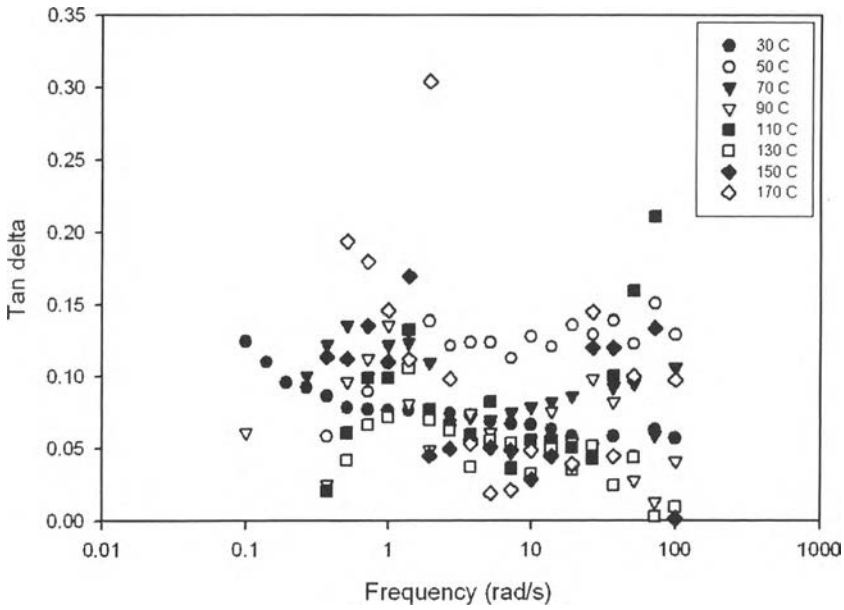

Figure 4.20 Tan δ of [Nylon12/NR]/[PS/NR/MA] with [PS/NR/MA] 2 phr content reactive blend at various temperature.

4.4.2 Effect of compatibilizer content in [Nylon12/NR]/Compatibilizer blends

The [Nylon12/NR]/[PS/NR] blends with variation in [PS/NR] content showed the increasing dispersed phase size with increasing [PS/NR] content in the blends (Appendix C, Figure C12 and C13).

TEM micrograph shows only inclusion of PS (core) in rubber particle (shell) in [Nylon12/NR]/[PS/NR] blend compared with the [Nylon12/NR]/SEBS G1650 blend morphology. This should attribute to the excellent compatibility of NR phase in the bulk and in [PS/NR] (Appendix C, Figure C14).

The effects of compatibilizer content on storage modulus, loss modulus and tan δ were shown in Figures 4.21, 4.22, and 4.23, respectively. Theses figures were obtained from [Nylon12/NR]/[PS/NR] reactive blend at 30°C. With increasing the compatibilizer content, storage modulus and loss modulus increased initially and decreased continuously. The [Nylon12/NR]/[PS/NR] with [PS/NR] 2

phr have the highest storage modulus and loss modulus compared with other [PS/NR] contents due to the inclusion of PS core, high amount of Nylon12 crystalline, and proper dispersed size. Increasing compatibilizer content provides less crystallinity of Nylon12 and more amorphous content leading to lower modulus. The worse case is occurred at loading of 16 phr where the storage modulus is lower than the blend without compatibilizer. However, storage modulus increases with frequency or stronger for the fast imposed load. Besides, adding PS/NR results in increasing loss modulus more than that of the simple binary blend except the loading of 16 phr. There are not much different in loss modulus among the blend with PS/NR 1-8 phr; however, the values are large at low frequency indicating the high energy dissipation with longer time. Therefore, the relaxation of chains is insignificant different by different loading.

At lower content of [PS/NR], [Nylon12/NR]/[PS/NR] with 1 phr [PS/NR], the dispersed phase size is lower than 2 phr [PS/NR] content. However, storage modulus of 1 phr [PS/NR] content lower than storage modulus of 2 phr [PS/NR] content due to lower PS (rigid part) content. At higher [PS/NR] contents, (4, 8, and 16 phr [PS/NR]), storage modulus decreased continuously due to the increasing of particle size and more content of NR with the assumption that when NR content increases (by the addition of PS/NR), NR tends to stay together due to decreasing in storage modulus.

From Figure 4.23, [Nylon12/NR]/[PS/NR] with [PS/NR] 2 phr blend has the lowest tan δ compared with other [PS/NR] contents. This figure indicates that [Nylon12/NR]/[PS/NR] with [PS/NR] 2 phr blend has a rigid structure due to the highest storage modulus.

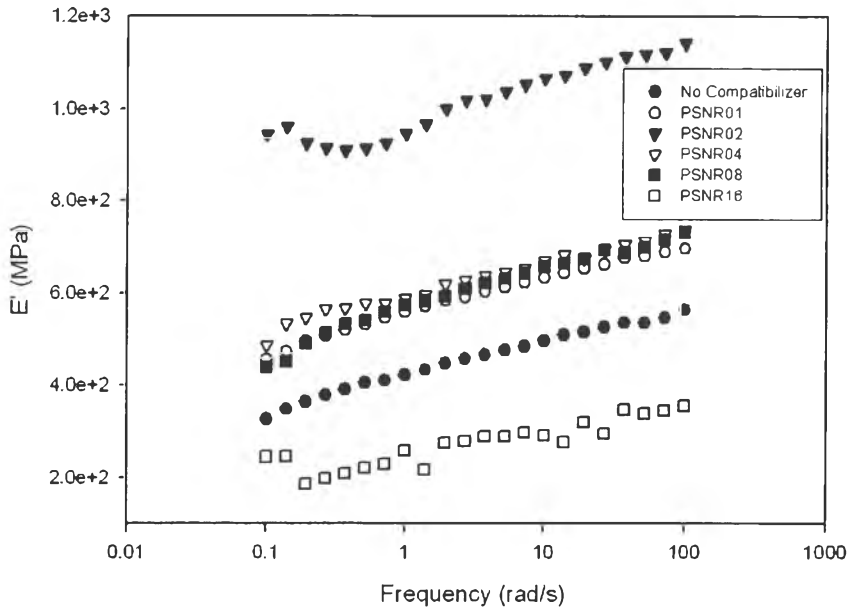

Figure 4.21 Storage modulus of [Nylon12/NR]/[PS/NR] reactive blends at 30°C with various [PS/NR] contents.

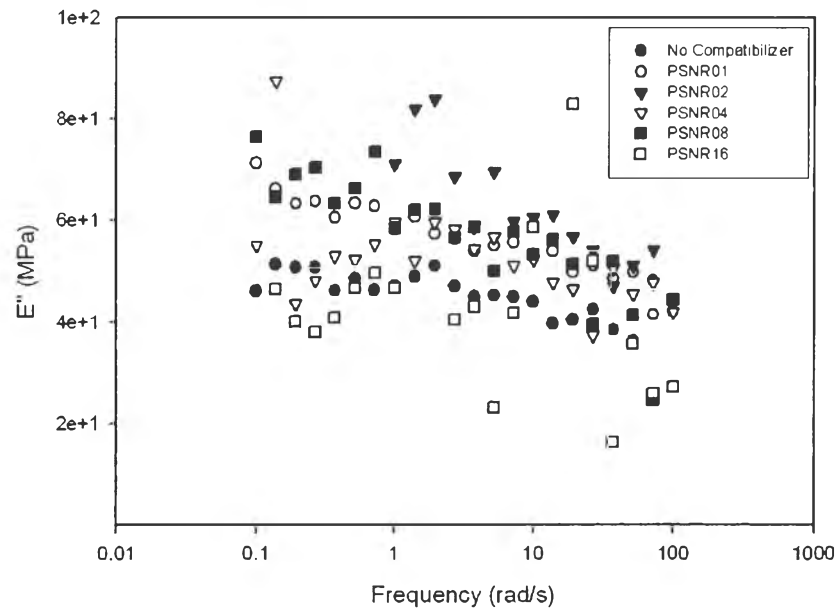

Figure 4.22 Loss modulus of [Nylon12/NR]/[PS/NR] reactive blends at 30°C with various [PS/NR] contents.

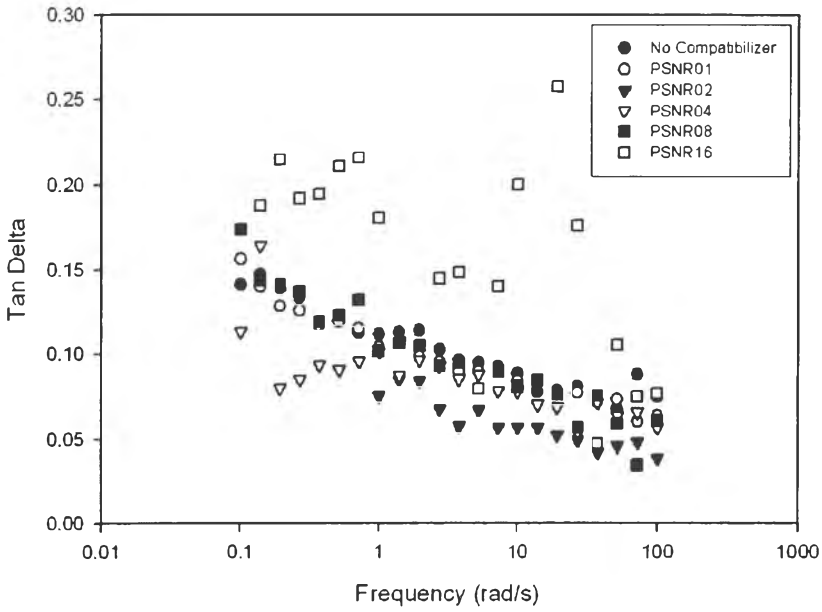

Figure 4.23 Tan δ of [Nylon12/NR]/[PS/NR] reactive blends at 30°C with various [PS/NR] contents.

Figures 4.24, 4.25, and 4.26 showed the effect of compatibilizer content on storage modulus, loss modulus and tan δ, respectively, of [Nylon12/NR]/[PS/NR/MA] reactive blend at 30°C. PS/NR/MA compatibilizer showed the same result as PS/NR, and the [Nylon12/NR]/[PS/NR/MA] with [PS/NR/MA] 2 phr has the highest storage modulus and loss modulus compared with other [PS/NR/MA] contents.

At higher [PS/NR/MA] contents, (4, 8, 16 phr [PS/NR/MA]), storage modulus decreased continuously due to lower crystallinity of Nylon12 matrix, the increasing of particle size and NR content. The loss moduli for PS/NR/MA compatibilizer were comparble to those of PS/NR compatibilizer and rather steady among several loading levels and frequency indicating stable morphology; however, the highest loss modulus is at 2 phr.

From Figure 4.26, [Nylon12/NR]/[PS/NR/MA] with [PS/NR/MA] 2 phr blend has the lowest tan δ compared with other [PS/NR/MA] contents. This figure indicates that [Nylon12/NR]/[PS/NR/MA] with [PS/NR/MA] 2 phr blend has a rigid structure due to the highest storage modulus. Tan δ of the blends with

PS/NR/MA 8-16 phr are relatively high suggesting the morphology is easier to be deformed especially at both extreme of low and high frequencies and hence they are not strong and durable. On the other hand, the blends with 1-4 phr have low tan δ comparable to those of PS/NR.

The molecular motions of the blends with 1-4 phr PS/NR or PS/NR/MA are not much different and such there mechanical properties are similar with the optimum about 2 phr. However, at loading of 8-16 phr, the molecular motion or energy dissipation (tan δ) are more facilitated especially at high frequency making the tensile and impact strengths drop very fast.

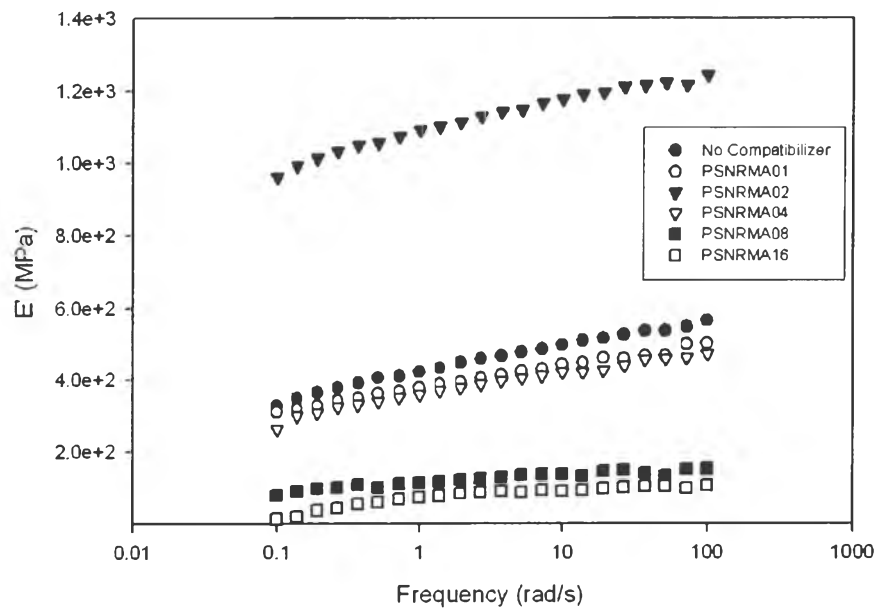

Figure 4.24 Storage modulus of [Nylon12/NR]/[PS/NR/MA] reactive blends at 30°C with various [PS/NR/MA] contents.

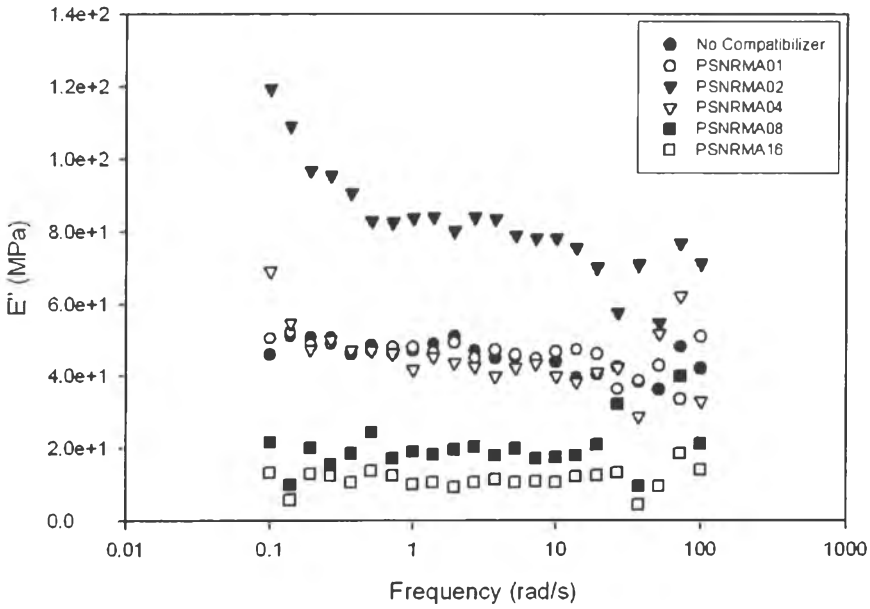

Figure 4.25 Loss modulus of [Nylon12/NR]/[PS/NR/MA] reactive blends at 30°C with various [PS/NR/MA] contents.

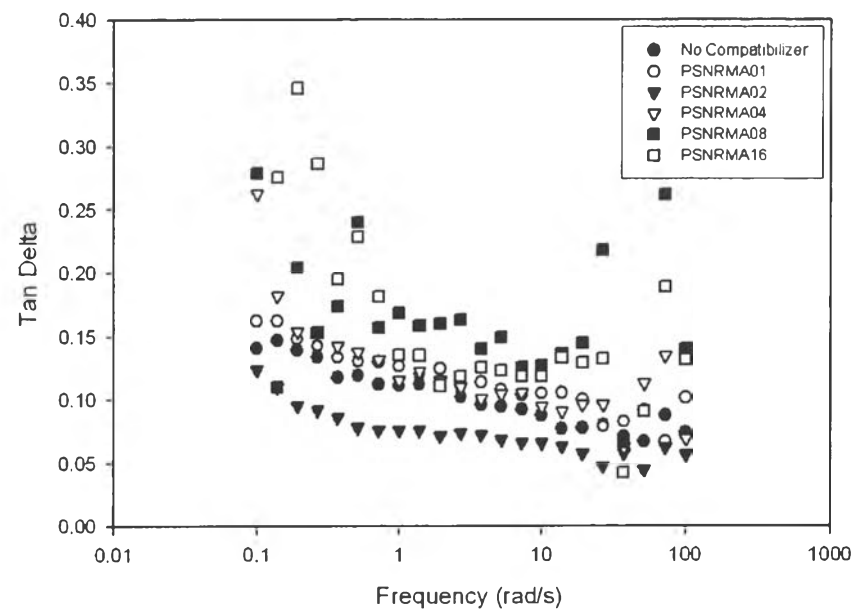

Figure 4.26 Tan δ of [Nylon12/NR]/[PS/NR/MA] reactive blends at 30°C with various [PS/NR/MA] contents.

4.4.3 Effect of type of Compatibilizer in [Nylon12/NR]/ Compatibilizer blends

4.4.3.1 Effect of SEBS and reactive SEBS in blends

The effect of simple SEBS and SEBS-g-MA were compared. The cryogenic fracture of the blends was observed by SEM after etching NR and SEBS phase by toluene (90%wt toluene/10%wt IPA for SEBS-g-MA). The dispersed phase size of [Nylon12/NR]/SEBS G1652 blends was increased with increasing the SEBS content. The shape of the dispersed phase is irregular and become more spherical for the blends after addition of 1 phr SEBS. The number average of dispersed phase size measurement was estimated by averaging the diameter of about 100 domains randomly for each blend system. However, the average diameter decreased with increasing SEBS-g-MA content, the [Nylon12/NR]/SEBS FG1901X blends showed a reduction in dispersed phase size and then levels off at the higher concentration. This levelling point could be considered as the interfacial saturation point where the concentration of SEBS-g-MA in [Nylon12/NR]/SEBS FG1901X was high enough to saturate the interface between Nylon12 and NR to produce perfect core-shell formation (Appendix C, Figures C9 and C10).

The effect of reactive functional group of compatibilizer on storage modulus, loss modulus and tan δ were shown in Figures 4.27, 4.28, and 4.29, respectively. The [Nylon12/NR]/SEBS G1652 showed higher storage modulus and loss modulus than [Nylon/NR]/SEBS FG 1901X, see Figure 4.27 and Figure 4.28. This indicates that although SEBS FG 1901X provides better phase adhesion than SEBS G1652, it does not mean better storage modulus, too. This attributes to effect of morphology. Based on TEM micrograph, (Appendix C, Figure C3), it show the Nylon12 core (rigid phase) and NR shell morphology with SEBS G1652 at the interface larger than dispersed phase with SEBS FG 1901X. The rigidity of large size core gives the high modulus. Moreover, loss moduli give the same trend as found for storage moduli; however, at low frequency or long time the SEBS allow more molecular energy dissipation than that of SEBS-MA. This suggests that SEBS FG 1901X gives strong interaction between two phases while the blend with SEBS G 1652 shows more chain mobility. Tan δ in Figure 4.29 gives better information for

the molecular mobility and strength of materials. In this case, SEBS is more effective than SEBS-MA to lower energy dissipation such even at long time indicating chain rigidity plays important role to improve strength rather than specific interaction. This is thus can be further investigated by using either SEBS with high molecular weight or high content of PS to verify this effect.

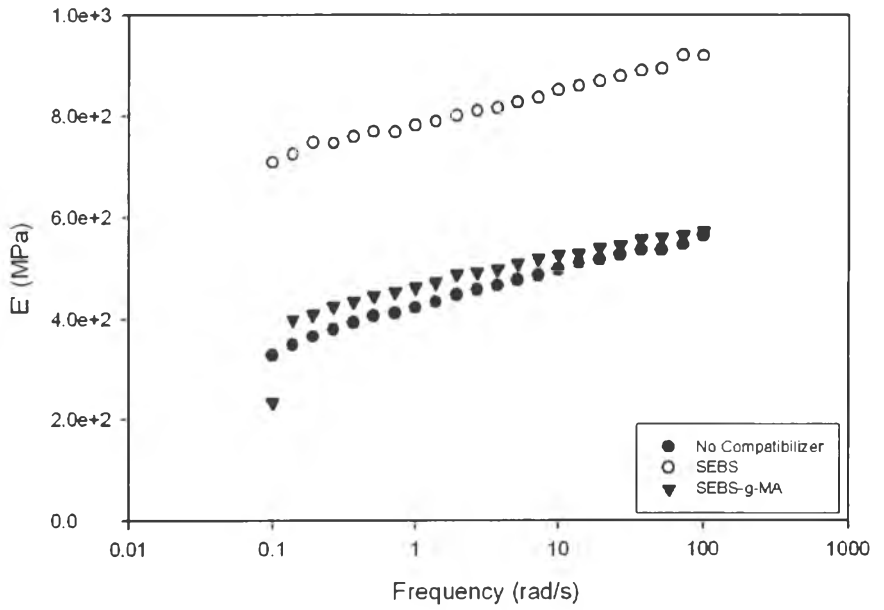

Figure 4.27 Storage modulus of [Nylon12/NR]/SEBS and [Nylon/NR]/SEBS-g-MA at 2 phr and 30°C.

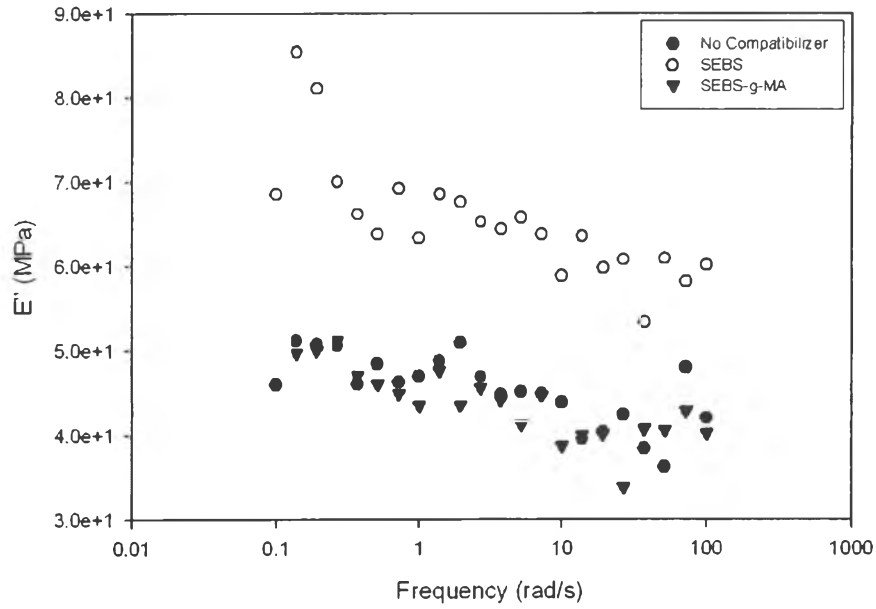

Figure 4.28 Loss modulus of [Nylon12/NR]/SEBS and [Nylon/NR]/SEBS-g-MA at 2 phr and 30°C.

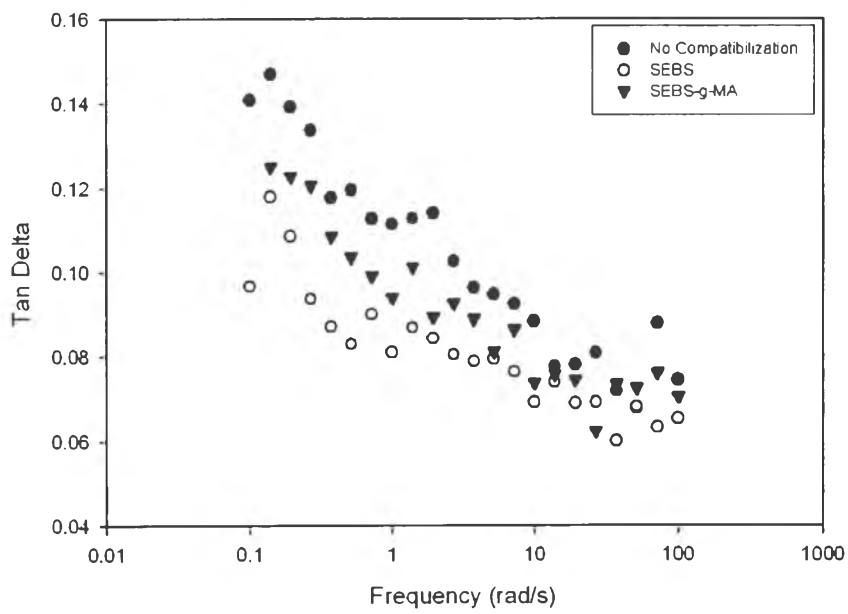

Figure 4.29 Tan δ of [Nylon12/NR]/SEBS and [Nylon/NR]/SEBS-g-MA at 2 phr and 30°C.

4.4.3.2 Effect of molecular weight of SEBS in blends

Dispersed phase size of [Nylon12/NR]/SEBS G1650 with variation in SEBS content showed the increasing dispersed phase size as increasing SEBS content very similar to that found in the blend with SEBS G1652. It was interesting to see that the particle sizes of these blends having SEBS G1650 less than 8 phr were relatively smaller than those of the blends with SEBS G1652. This showed the contribution of longer compatibilizer chain to enhance homogeneity, stabilized the interface and morphology and prevent coalescence. When more SEBS G1650 was added, the particle size and its distribution increased and larger than that of SEBS G1652 (Appendix C, Figures C4 and C5).

The effects of molecular weight of compatibilizer on storage modulus, loss modulus and tan δ were shown in Figure 4.30, 4.31, and 4.32, respectively. The [Nylon12/NR]/SEBS G1650 (High MW) showed a slightly higher storage modulus and loss modulus than [Nylon/NR]/SEBS G 1652 (Low MW), see Figure 4.30 and Figure 4.31. The result corresponded to the decrease in particle size of the blends with SEBS G 1650 indicating the better adhesion of the two phases due to longer chain of SEBS. Moreover, tan δ of [Nylon12/NR]/SEBS G1650, see Figure 4.32, slightly lower than that of [Nylon/NR]/SEBS G 1652, due to rigidity of SEBS chain with higher molecular weight. Moreover, at long time (low frequency), the low MW SEBS clearly shows greater chain mobility or energy dissipation than high MW SEBS.

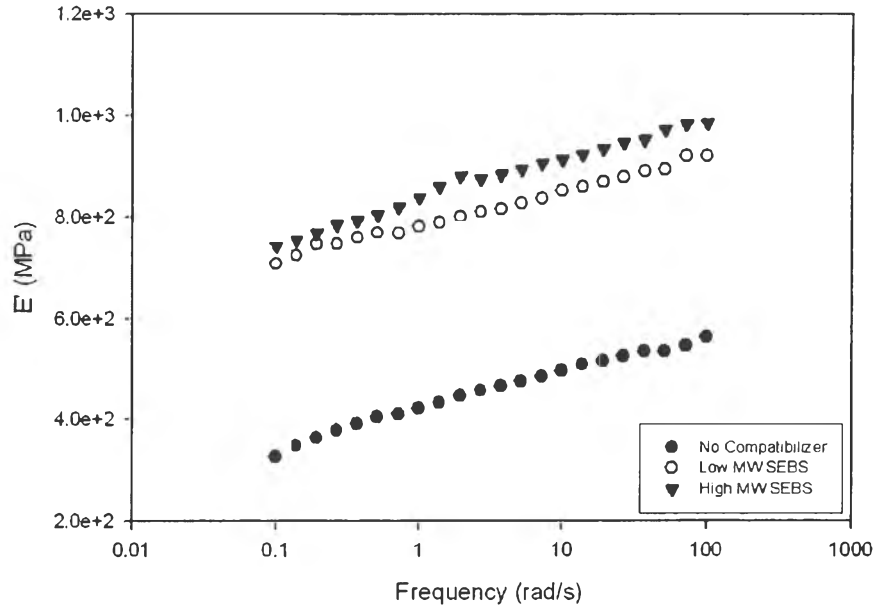

Figure 4.30 Storage modulus of [Nylon12/NR]/SEBS G 1652 (Low MW SEBS) and [Nylon12/NR]/SEBS G 1650 (High MW SEBS) at 2 phr and 30°C.

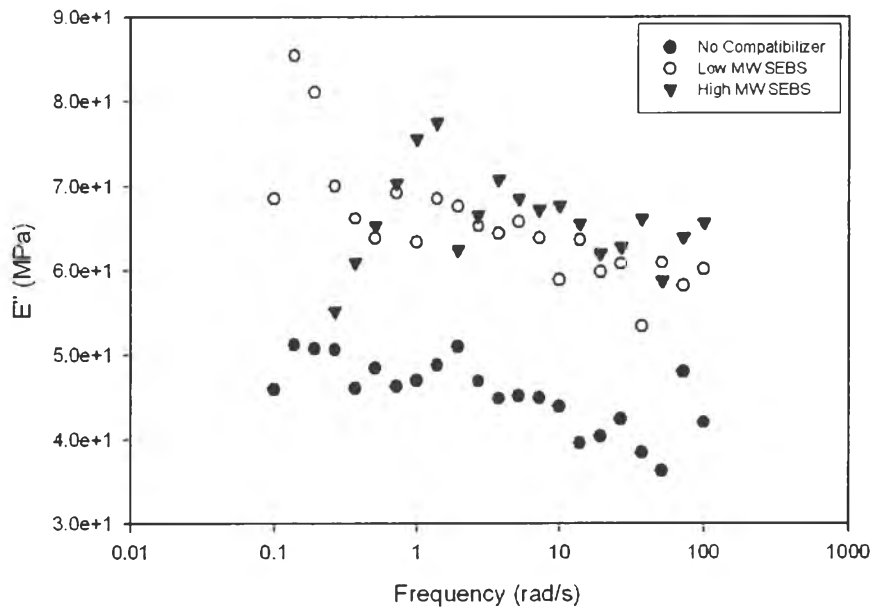

Figure 4.31 Loss modulus of [Nylon12/NR]/SEBS G 1652 (Low MW SEBS) and [Nylon12/NR]/SEBS G 1650 (High MW SEBS) at 2 phr and 30°C.

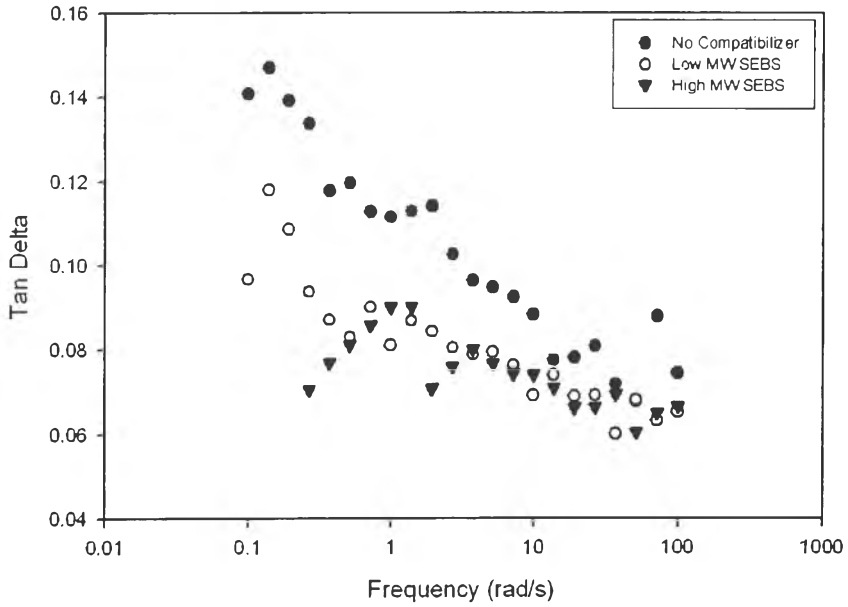

Figure 4.32 Tan δ of [Nylon12/NR]/SEBS G 1652 (Low MW SEBS) and [Nylon12/NR]/SEBS G 1650 (High MW SEBS) at 2 phr and 30°C.

4.4.3.3 Effect of %wt PS of SEBS in blends

The [Nylon12/NR]/SEBS G1657 blends with variation in SEBS content also showed the increasing dispersed phase size with increasing SEBS content as found in blends with SEBS G1652. The Nylon12 core size was obviously reduced with a thick rubber shell as a result of low PS content (Appendix C, Figure C7, C8 and C9).

The effects of %wt PS of SEBS on storage modulus, loss modulus and tan δ were shown in Figures 4.33, 4.34, and 4.35, respectively. The [Nylon12/NR]/SEBS G1650 (High %wt PS) showed a higher storage modulus than [Nylon/NR]/SEBS G 1657 (Low %wt PS), see Figure 4.32, due to higher PS content (rigid part). Moreover, tan δ of [Nylon12/NR]/SEBS G1650, see Figure 4.35, lower than [Nylon/NR]/SEBS G 1657, due to rigidity of SEBS chain.

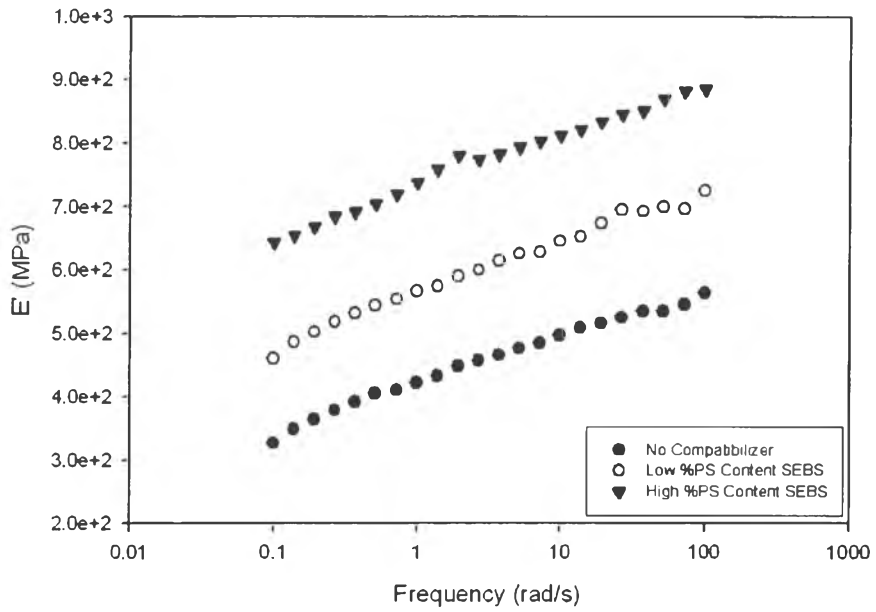

Figure 4.33 Storage modulus of [Nylon12/NR]/SEBS G 1650 (High %wt PS SEBS) and [Nylon12/NR]/SEBS G 1657 (Low %wt PS SEBS) at 2 phr and 30°C.

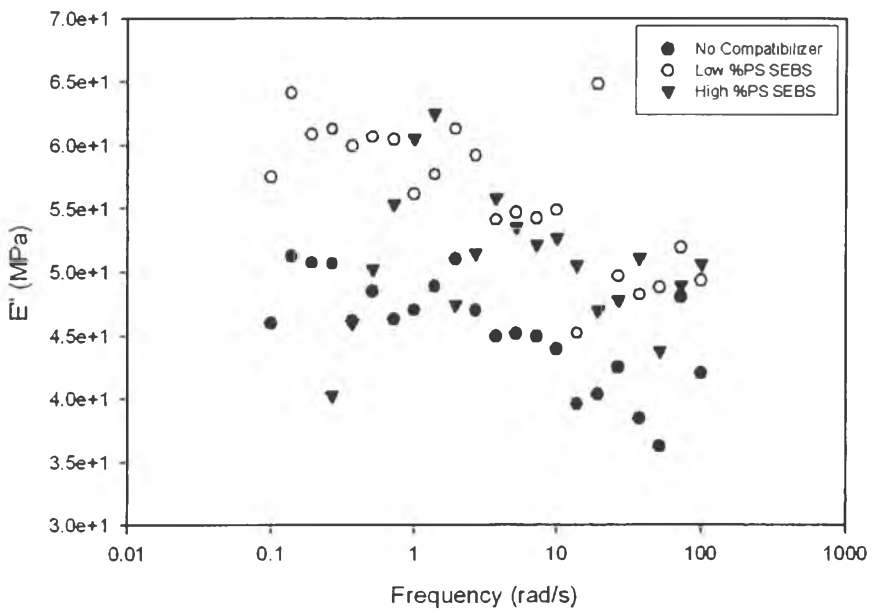

Figure 4.34 Loss modulus of [Nylon12/NR]/SEBS G 1650 (High %wt PS SEBS) and [Nylon12/NR]/SEBS G 1657 (Low %wt PS SEBS) at 2 phr and 30°C.

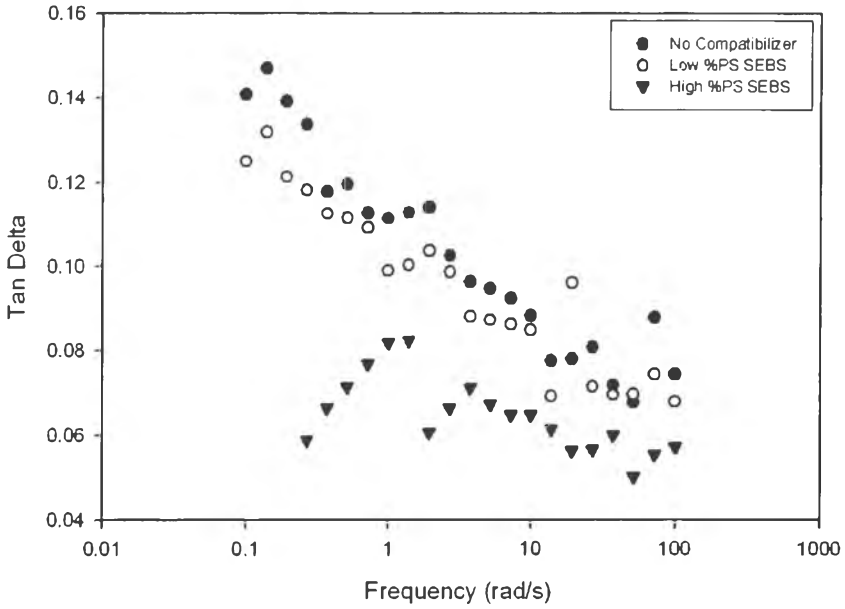

Figure 4.35 Tan δ of [Nylon12/NR]/SEBS G 1650 (High %wt PS SEBS) and [Nylon12/NR]/SEBS G 1657 (Low %wt PS SEBS) at 2 phr and 30°C.

4.4.3.4 Effect of [PS/NR] in the blends

The effects of PS/NR blend prepared by reactive processing on storage modulus, loss modulus and tan δ in comparison to SEBS with high MW and high PS content are shown in Figures 4.36, 4.37, and 4.38, respectively. The [Nylon12/NR]/[PS/NR] showed a higher storage modulus than [Nylon/NR]/SEBS G 1650, see Figure 4.36. The [PS/NR] reactive blends contain 60%PS which was double the content of PS in SEBS G 1650 but its MW was not known and was assumed to be more than 100,000 because MW of NR is generally 500,000. Moreover, PS/NR contains some gel making it high MW. Thus the content of soft NR phase was significantly reduced. Consequently, the PS hard segment (60%PS) and NR crosslinking contributed to the higher modulus of this blend compared to the other. Moreover, tan δ of [Nylon12/NR]/[PS/NR] ,see Figure 4.38, is also lower than [Nylon/NR]/SEBS G 1650.

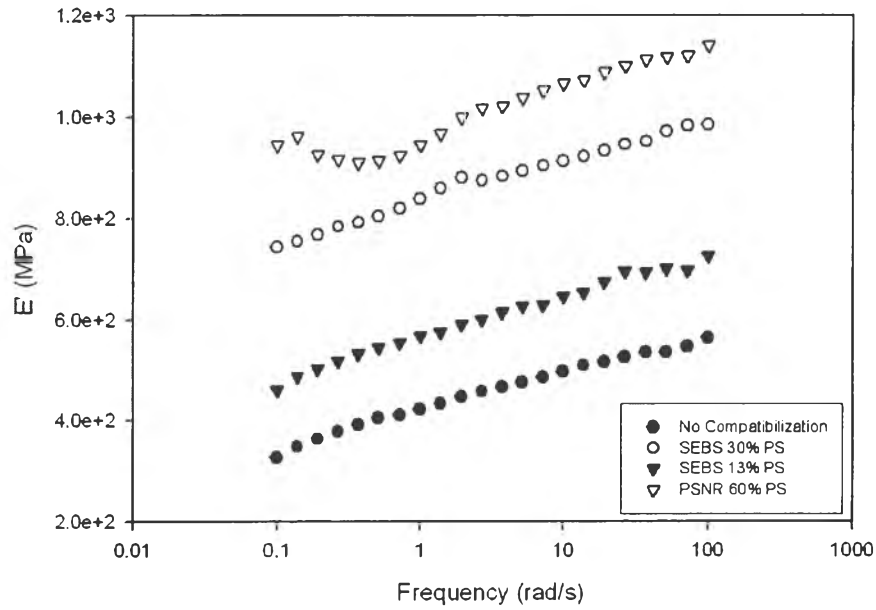

Figure 4.36 Storage modulus of [Nylon12/NR]/[PS/NR] (60% PS), [Nylon12/NR]/ SEBS G 1650 (30% PS) and [Nylon12/NR]/SEBS G 1657 (13% PS) at 2 phr and 30°C.

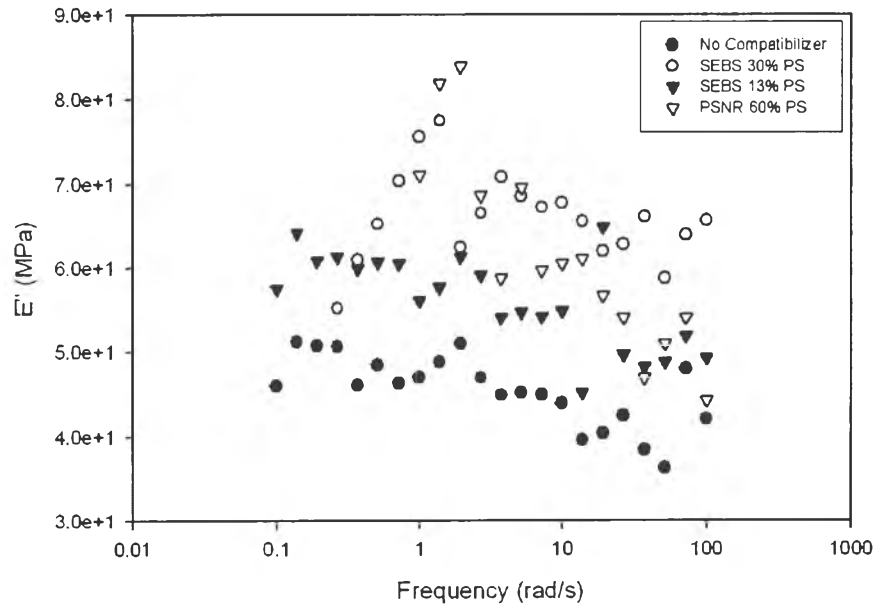

Figure 4.37 Loss modulus of [Nylon12/NR]/[PS/NR] (60% PS), [Nylon12/NR]/ SEBS G 1650 (30% PS) and [Nylon12/NR]/SEBS G 1657 (13% PS) at 2 phr and 30°C.

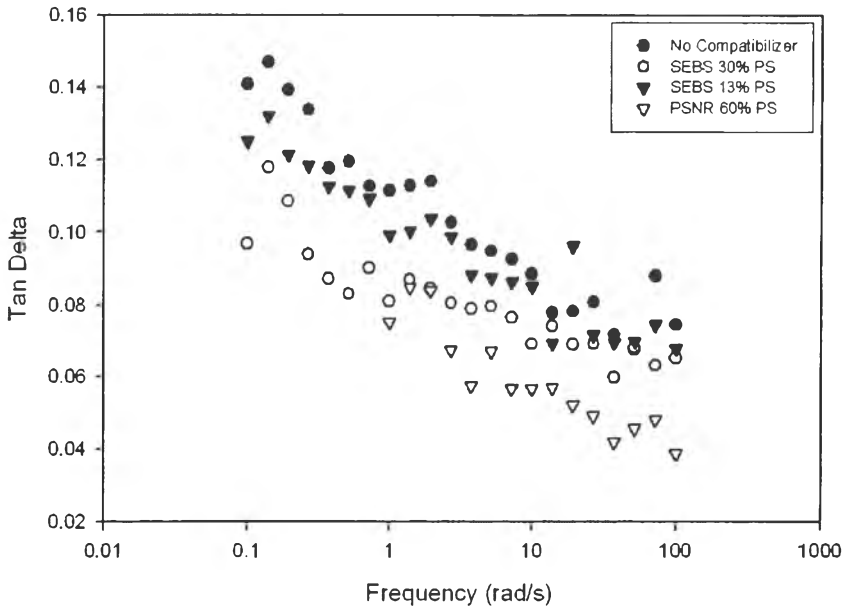

Figure 4.38 Tan δ of [Nylon12/NR]/[PS/NR] (60% PS), [Nylon12/NR]/SEBS G 1650 (30% PS) and [Nylon12/NR]/SEBS G 1657 (13% PS) at 2 phr and 30°C.

4.4.3.5 Effect of [PS/NR/MA] reactive blends in blends

The effect of PS/NR/MA reactive blends on storage modulus, loss modulus and tan δ are shown in Figures 4.39, 4.40, and 4.41, respectively. The [Nylon12/NR]/[PS/NR/MA] showed a higher storage modulus than [Nylon/NR]/[PS/NR] and [Nylon12/NR]/[FG1901X], see Figure 4.39. The [PS/NR/MA] reactive blends contain maleic anhydride which act as reactive agent compared with [PS/NR] reactive blends thus [PS/NR/MA] reactive blends have higher storage modulus than [PS/NR] reactive blends.

In addition, the [Nylon12/NR]/[PS/NR/MA] have the PS hard segment (60%PS) more than [Nylon12/NR]/[FG1901X] contributed to the higher modulus. However, loss modulus and tan δ of [Nylon12/NR]/[PS/NR/MA], see Figure 4.41, are about the same order or slightly greater than [Nylon12/NR]/[PS/NR] but lower than the others. This suggests easier energy dissipation has occurred to the reactive blend with PS/NR/MA than that with PS/NR. The large particle size in the blend with PS/NR/MA is contributed to more energy dissipation, especially at low frequency and longer time.

It should be noted that both PS/NR and PS/NR/MA contain toluene-insoluble gel of about 25%wt and 41 %wt, respectively. According to the storage moduli of blends containing both compatibilizers, the plateau modulus at long time was found only for the blend with PS/NR but not for PS/NR/MA or SEBS-MA which keep reducing storage modulus with time. The plateau modulus informs that the relaxation or mobility of the molecules is retarded. The increase in toluene-insoluble gel may be due to the incorporation of MA making the blend less soluble in toluene.

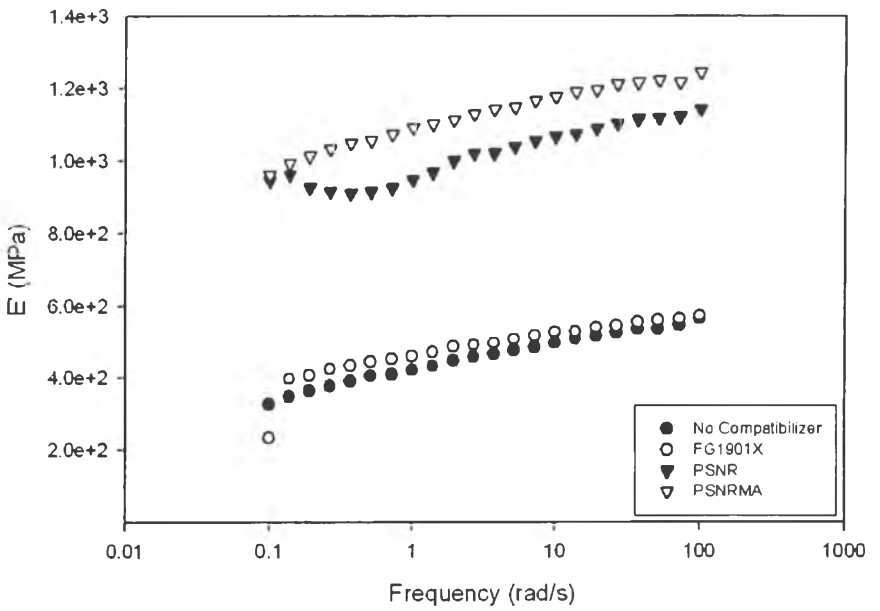

Figure 4.39 Storage modulus of [Nylon12/NR]/[PS/NR/MA], [Nylon12/NR]/[PS/NR], and [Nylon12/NR]/[FG1901X] at 2 phr and 30°C.

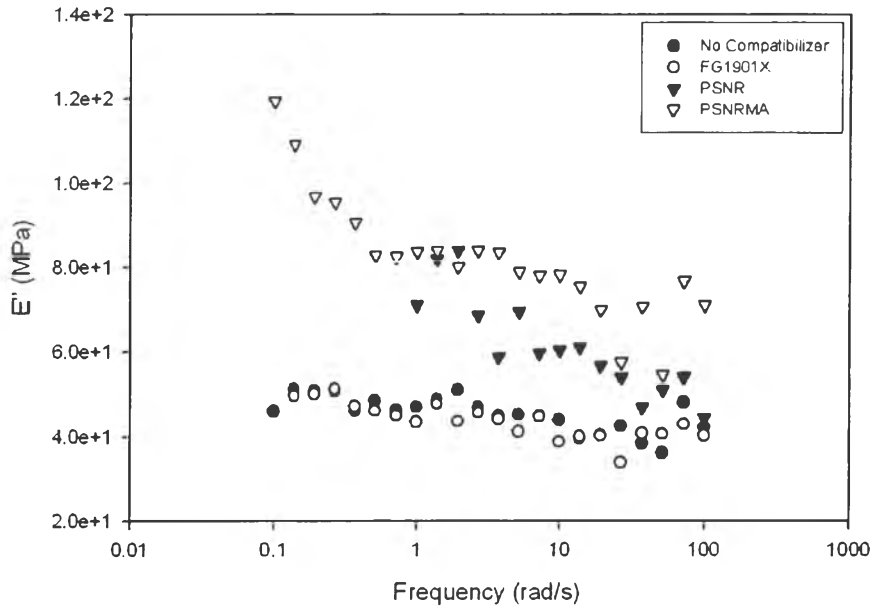

Figure 4.40 Loss modulus of [Nylon12/NR]/[PS/NR/MA], [Nylon12/NR]/[PS/NR], and [Nylon12/NR]/[FG1901X] at 2 phr and 30°C.

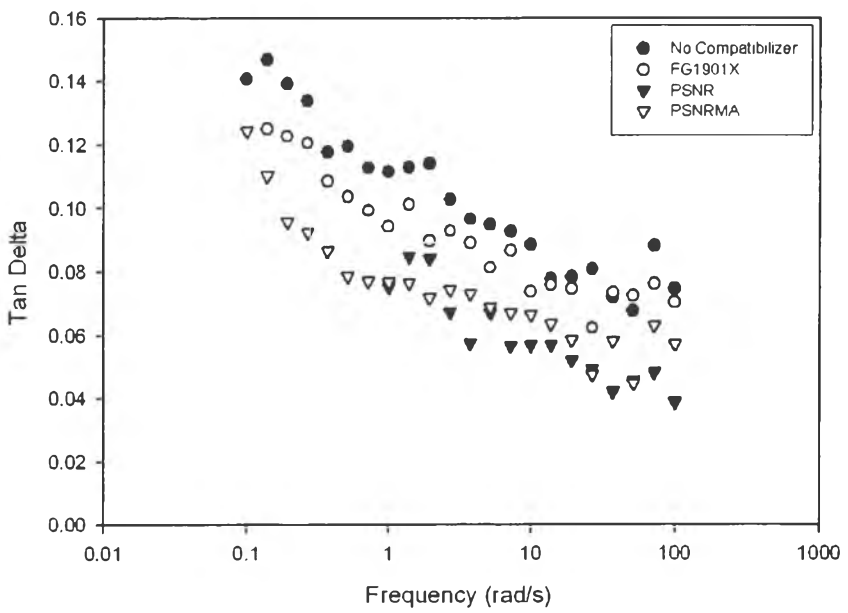

Figure 4.41 Tan δ of [Nylon12/NR]/[PS/NR/MA], [Nylon12/NR]/[PS/NR], and [Nylon12/NR]/[FG1901X] at 2 phr and 30°C.